IEEE Access
Multidisciplinary ⋮ Rapid Review ⋮ Open Access Journal

Received 9 November 2023, accepted 28 November 2023, date of publication 1 December 2023,
date of current version 11 December 2023.

Digital Object Identifier 10.1109/ACCESS.2023.3339057

RESEARCH ARTICLE

Improving the Security and Reliability of Energy-Constrained Two-Way Relay Systems With Nonlinear Energy Harvesting

ENYU LI, (Member, IEEE), YE WANG, ZANYANG LIANG, AND MEIJUAN ZHENG
School of Information and Control Engineering, Qingdao University of Technology, Qingdao 266520, China

Corresponding author: Enyu Li (lienyu0123@163.com)

This work was supported in part by the Natural Science Foundation of Shandong Province, China, under Grant ZR2022MF273 and Grant ZR2020MF001; and in part by the National College Students Innovation and Entrepreneurship Training Program, China, under Grant S202210429170, Grant S202310429182, and Grant S202310429489.

ABSTRACT This paper presents a novel three-time slot transmission protocol designed for energy-constrained two-way relay systems. In a departure from traditional energy sources, our approach serves a dual purpose by not only providing power to the system but also significantly enhancing its security. We leverage both physical-layer network coding (PNC) and bit-level Exclusive OR (XOR) technology to amplify system capacity and bolster security. Given the unavailability of exact closed-form solutions, we utilize tight upper bounds for the signal-to-noise ratio (SNR) to derive approximate closed-form results, specifically focusing on outage and intercept performance under Rayleigh channel conditions. We also provide performance bounds for outage and intercept probabilities in the high SNR regime. Our simulation results validate the accuracy of our derived probabilities, demonstrating consistency with Monte Carlo simulations. Furthermore, our investigation reveals that the time allocation factor has minimal impact on the security and reliability of the proposed protocol, particularly under high SNR conditions. In addition, we conduct a comparative analysis between the XOR scheme introduced in this article and non-XOR (NXOR) systems. This analysis underscores the superior security-reliability tradeoff of our approach, particularly in scenarios characterized by poor channel conditions between the energy source user and potential eavesdroppers.

INDEX TERMS Two-way relay, energy harvesting, physical-layer network coding, cooperative communications, Rayleigh channel.

I. INTRODUCTION

Wireless communication technology has developed rapidly in recent years, and along with the rapid iteration of various smart terminal devices, a variety of new communication services have emerged, which are not only computationally intensive but consume much more energy than the last few generations of mobile communication technology. However, due to the bottleneck in the development of energy storage technology such as batteries, which leads to mobile devices will be limited by the limitations of battery technology. The energy harvesting (EH) technology can improve the energy efficiency of communication networks with limited processing power and low-power energy constraints, and can effectively alleviate the conflict between the power demand of mobile communication devices and battery energy storage [1], [2], [3], [4]. Simultaneous wireless information and power transfer (SWIPT) is a method that enables simultaneous EH and information transfer, which generally uses signal splitting to achieve synchronization of energy collection and information decoding. To facilitate wireless information and power transfer at the receiver, two practical receiver architecture designs are proposed, namely power-splitting (PS) and time-switching (TS) [5], [6]. Perera et al. [7] and Zewde et al. [8] have investigated the EH non-orthogonal multiple access (NOMA) and

The associate editor coordinating the review of this manuscript and approving it for publication was Jie Tang.

SWIPT-NOMA systems, respectively, to explore the problem of solving the system's energy efficiency and spectrum utilization. Linear EH problems have been studied more in ideal scenarios, while nonlinear EH has been more studied as a more generalized research problem. Ma et al. [9] investigated the full-duplex (FD) relay model using the PS approach, simulating the outage probability performance of linear EH and nonlinear EH, thus demonstrating the superiority of the NOMA system under nonlinear EH. Maleki et al. [10] combined TS with PS and analyzed the performance of the hybrid EH protocol. Okandeji et al. [11] studied the performance of the FD-SWIPT system to achieve the maximum transmission rate of the system by controlling the power allocation factor, transmit power, and other conditions of the system but did not consider the relationship between system energy and rate. Boshkovska et al. [12] investigated the performance of rate-energy tradeoff at different signal-to-noise ratios (SNRs) based on the TS model to explore the optimal solution for transmission speed and energy reception. Zhang et al. [13], [14] conducted separate analyses of the outage performance of the system under both single EH mode and dual EH mode. They performed simulations to evaluate system performance in various environments, providing evidence that the proposed dual EH mode offers superior outage performance. Jiang et al. [15] calculated the optimal allocation ratio between EH and information detecting (ID) to determine the optimal trade-off between rate and energy for TS and PS modes under non-linear EH. Makhanpuri et al. [16] proposed a more practical TS-non-linear EH model in the FD mode and enhanced the performance of the far-end user by optimizing TS parameters. Maji et al. [17] discussed the security of information transmission under non-linear EH. However, their research revealed that when using the non-linear EH model, the system's security is not as strong as with the linear EH model.

Wireless communication cannot have the same high security and confidentiality as wired communication because of its broadcasting and sending characteristics, which leads to the security of wireless communication has been a hot issue of research. Besides improving transmission efficiency, physical-layer network coding (PNC) technology can also use the physical characteristics of the channel to ensure that the communication quality of the eavesdropping node is inferior to that of the legitimate user's channel, thus achieving the confidential transmission of information [18], [19], [20]. Recently, PNC technology has also been introduced by scholars into SWIPT technology, thus enabling the secure transmission of concurrent energy communication information [21], [22]. Dong et al. [23] conducted a study on the relationship between the transmit power of the base station and the user secrecy rate in the SWIPT system to explore the trade-off between the transmit power of the base station and the user secrecy rate. In the study of nonlinear SWIPT networks in [24], the security of information transmission was improved by adding artificial redundant signals to the transmitting signals. In contrast to the above methods, in [25], Khandaker et al. reduce the SNR received by the eavesdropper by adding artificial noise, thus achieving confidential communication.

Relay cooperative networks have the advantage of expanding signal coverage and improving communication quality, while two-way relaying can solve the communication delay problem by improving spectrum utilization [26]. In [27] and [28], two-way relaying is used to assist in the transmission of superimposed signals, thus reducing the time slot required for information transmission and reducing the time required for information transmission while ensuring transmission quality. The combination of two-way relaying with EH can reduce the time delay of signal communication and further improve the quality of communication networks while ensuring sufficient energy at the transmitter side, so it has excellent development prospects [29], [30], [31], [32]. Shah et al. [33] and Do et al. [34] investigate the models of two-way decode-and-forward (DF) relaying and two-way amplify-and-forward (AF) relaying combined with EH to study the outage probability problem under PS and TS, respectively, and compare the outage performance under different parameters.

From Table 1, it can be observed that in the research on energy-constrained systems, most studies have only considered PS or TS EH mode and have not addressed system security. Only a few studies have aimed to enhance system security by adding redundant signals or external artificial noise. However, these approaches often impose higher demands on devices, especially when adding external artificial noise, which may lead to increased operational costs for communication equipment. Additionally, research on the combination of two-way relaying and EH is limited, while non-linear EH combined with two-way relaying systems is more in line with real-world transmission scenarios. In response to these limitations, this paper introduces a novel approach that integrates bit-level Exclusive OR (XOR) and NOMA techniques. While augmenting the system's capacity, the information is encrypted from the physical layer aspect using XOR between the source signal and the user signal. Building upon this foundation, we conduct an investigation into a non-linear EH two-way AF relay system designed to facilitate efficient and secure data transmission over Rayleigh channels. This paper's primary contributions are summarized as follows:

- An EH two-way untrusted AF relay network is established, in which an independent energy source is introduced to guarantee the energy required for message transmission. Meanwhile, the PNC technology is used to encrypt the user's sending signal during the broadcasting stage to guarantee the security of information transmission.
- Based on the nonlinear EH model and the proposed data forwarding protocol, the tight upper bounds of SNR are used to derive the closed-form lower bound of outage

TABLE 1. Literature review on some related EH systems.

Ref.	Energy Harvesting	Access Scheme	Encryption method	Relay type	TS/PS
[8]	Linear EH	NOMA	N.A.	One-way	N.A.
[9]	Nonlinear EH	NOMA	N.A.	One-way	PS
[14]	Nonlinear EH	NOMA	N.A.	One-way	PS
[16]	Nonlinear EH	NOMA	N.A.	One-way	TS
[25]	Linear EH	N.A.	Artificial Noise	One-way	N.A.
[33]	Linear EH	N.A.	N.A.	Two-way	TS
Our work	Nonlinear EH	NOMA	XOR	Two-way	PS and TS

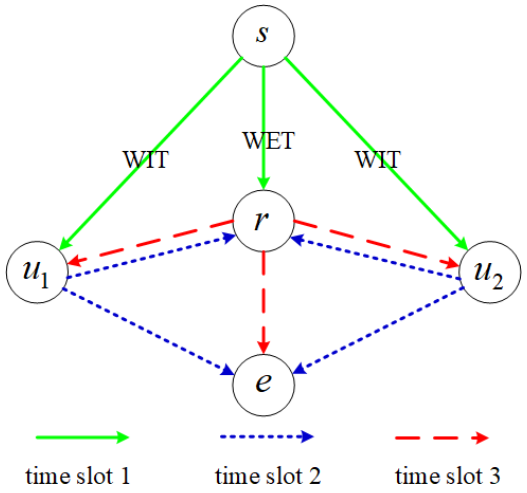

FIGURE 1. System model.

probability and upper bound of intercept probability. Then the approximate performance at high SNR was investigated.

- We discuss the metrics that affect the security and reliability performance of the system. The simulation results show that the time allocation factor of the system has almost no effect on the system outage probability and intercept probability. Finally, compared with the non-XOR (NXOR) protocol, simulation results demonstrate the superiority of the proposed protocol.

II. SYSTEM MODEL

In order to enable two users to exchange data with energy-constrained untrusted relay and to improve the security of the exchanged data, a system model as shown in Fig.1. is developed, in which WIT and WET respectively represent wireless information transfer and wireless energy transfer. In this model, the distance between two users u_1 and u_2 is too far to communicate directly, and an energy-constrained two-way AF relay r must be used to enable data exchange. To solve the problem of limited relay energy and to improve the security of the data exchanged between the two users u_1 and u_2, an independent energy source s is introduced, which serves both to provide encrypted data to users and provide energy to the relay r. The eavesdropper e is far from s, not able to receive or only able to receive a weak signal

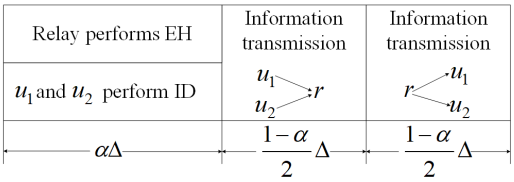

FIGURE 2. The proposed 3-time slot transmission protocol.

sent by s, mainly eavesdropping on the data exchanged by the two users. In this model, each node is a single antenna device and operates in half-duplex mode. The channels between any two points i and j are denoted by h_{ij} and obey independent flat Rayleigh fading with zero mean and variance σ_{ij}^2. The different channels are independent of each other and each channel has symmetry and satisfies $h_{ij} = h_{ji}$. The noise received by any node j is denoted by n_j and is all additive white Gaussian noise (AWGN) with zero mean and variance N_0. It is further assumed that each node knows the channel state information (CSI) associated with itself.

A. FORWARDING PROTOCOL AND SIGNAL MODEL

For this model, to achieve a secure and reliable data exchange between two users, a 3-time slot transmission protocol is designed as shown in Fig.2. The first time slot is the phase of ID and EH for the two users and the relay, respectively, and the occupied duration is $\alpha\Delta$, where Δ is the duration to complete one data exchange and α is the time allocation factor for ID and EH, satisfying $\alpha \in (0, 1)$. The second time slot is the multi-access phase for two users, and the third time slot is the relay forwarding phase, both of which are occupied for a duration of $(1-\alpha)\,\Delta/2$. The specific forwarding process is as follows:

The first time slot: s transmits its signal x_s to u_1, u_2 and r, so the signal received by node τ ($\tau \in \{u_1, u_2, r\}$) can be expressed

$$y_{s\to\tau} = \sqrt{P_s} h_{s\tau} x_s + n_\tau, \tag{1}$$

where P_s is the average transmitting power of source s, $E\left\{|x_s|^2\right\} = 1$, $E\{\bullet\}$ denotes the expectation. For the energy-constrained relay r, x_s is the energy signal, while for the two users u_1 and u_2, x_s is the signal which can be used to encrypt the data forwarded by these two users, namely, secret key.

The second time slot: The two users demodulate x_s and convert it into binary bitstream data, which is represented by s_s. Then u_i ($i \in \{1,2\}$) performs PNC on the data s_i, which will be sent to u_j ($j \in \{1,2\}, j \neq i$) by u_i, that is, u_i performs bit-level XOR processing to obtain $s_i' = s_i \oplus s_s$, where $\oplus$ represents bit-level XOR. Then the two users u_1 and u_2 convert the binary bitstream data s_1' and s_2' into modulated signals x_1' and x_2', respectively, and broadcast them at the same time. At this time the relay r and eavesdropper e received the signal as

$$y_{u_1,u_2\to\upsilon} = \sqrt{P_{u_1}} h_{u_1\upsilon} x_1' + \sqrt{P_{u_2}} h_{u_2\upsilon} x_2' + n_\upsilon, \tag{2}$$

where $\upsilon \in \{r, e\}$, P_{u_1} and P_{u_2} are the average transmit power of the two users u_1 and u_2, respectively. Similarly, $E\left\{\left|x_1'\right|^2\right\} = E\left\{\left|x_2'\right|^2\right\} = 1$.

The third time slot: The relay amplifies the received signal $y_{u_1,u_2\to r}$ with the amplification factor β, which can be expressed as

$$\beta = \sqrt{\frac{P_r}{P_{u_1}\left|h_{u_1 r}\right|^2 + P_{u_2}\left|h_{u_2 r}\right|^2 + N_0}}, \tag{3}$$

where P_r is the average transmit power of the relay. Then the relay will broadcast the amplified signal, at this time the user υ ($\upsilon \in \{u_1, u_2, e\}$) receives the signal as

$$\begin{aligned} y_{r\to\upsilon} &= h_{r\upsilon}\beta y_{u_1,u_2\to r} + n_\upsilon \\ &= \sqrt{P_{u_1}}\beta h_{ru_1}h_{r\upsilon}x_1' + \sqrt{P_{u_2}}\beta h_{ru_2}h_{r\upsilon}x_2' + \beta h_{r\upsilon}n_r + n_\upsilon \end{aligned} \tag{4}$$

B. NON-LINEAR EH MODEL

Compared with the power of transmit signal by s, the power of AWGN received by r is much smaller, so the AWGN can be ignored during the EH process. Therefore, from (1), we known that the input power available in the process of EH for the relay r is

$$P_{in} = P_s|h_{sr}|^2. \tag{5}$$

Considering the effect of nonlinear characteristics in the actual EH process, the EH circuit does not harvest any energy when the input power P_{in} is below the sensitivity value $P_{\min}$. When the input power is greater than $P_{\min}$, the EH circuit harvests energy in a linear relationship, but when it reaches the saturation value P_{th}, the input power of the energy harvester becomes a constant value P_{th}. Thus, the energy that can be harvested by relay r during the first time slot is

$$E_{in} = \begin{cases} 0, & P_{in} < P_{\min} \\ P_s|h_{sr}|^2\alpha\Delta, & P_{\min} < P_{in} \le P_{th} \\ P_{th}\alpha\Delta, & P_{in} > P_{th} \end{cases}. \tag{6}$$

All the harvested energy is used to amplify and forward the signals of the two users received in the third time slot. Since the duration of the third time slot is $(1-\alpha)\Delta/2$, the mathematical model of the average transmit power when r amplifies and forwards data can be expressed as

$$P_r = \begin{cases} 0, & P_{in} < P_{\min} \\ \dfrac{2\eta P_s|h_{sr}|^2\alpha}{1-\alpha}, & P_{\min} < P_{in} \le P_{th} \\ \dfrac{2\eta P_{th}\alpha}{1-\alpha}, & P_{in} > P_{th} \end{cases}, \tag{7}$$

where η is the energy conversion efficiency.

C. DECODING SITUATION ANALYSIS AND SNR MODEL

In the first time slot, from (1), it is known that the SNR of the user τ ($\tau \in \{u_1, u_2\}$) decoding x_s is

$$\gamma_\tau^{x_s} = \rho_s|h_{s\tau}|^2, \tag{8}$$

where $\rho_s = P_s/N_0$. Similarly, the latter $\rho_\kappa = P_\kappa/N_0$, $\kappa \in \{u_1, u_2, r, \min, th\}$.

Remark: The SNR is usually considered to be able to decode correctly when it is greater than the preset SNR threshold T. In general, the energy source s has a much higher transmitting power, so the probability of successful decoding x_s for these two users is high.

Due to the AF protocol is employed, the relay r does not need to decode any data in the second time slot. For the eavesdropper e, due to the random characteristics of the channel and considering the successive interference cancellation (SIC) technical principle of NOMA decoding requirements, the order in which e decodes x_1' and x_2' is divided into two cases.

Case 1: In the case of $P_{u_1}\left|h_{u_1 e}\right|^2 > P_{u_2}\left|h_{u_2 e}\right|^2$, the term containing x_2' in (2) is regarded as noise, when e decodes x_1' firstly. Then e eliminates the term containing x_1' and decode x_2'. In order to reduce the complexity of the performance analysis, the perfect SIC technique is considered here and the corresponding SNRs are

$$\gamma_{e2}^{x_1'} = \frac{\rho_{u_1}\left|h_{u_1 e}\right|^2}{\rho_{u_2}\left|h_{u_2 e}\right|^2 + 1}, \tag{9}$$

$$\gamma_{e2}^{x_2'} = \rho_{u_2}\left|h_{u_2 e}\right|^2. \tag{10}$$

Case 2: In the case of $P_{u_1}\left|h_{u_1 e}\right|^2 < P_{u_2}\left|h_{u_2 e}\right|^2$, first, e decodes the desired signal x_2' by treating x_1' as noise. After that, x_1' will be decoded by subtracting x_2' completely. The corresponding SNRs are

$$\gamma'^{x_2'}_{e2} = \frac{\rho_{u_2}\left|h_{u_2 e}\right|^2}{\rho_{u_1}\left|h_{u_1 e}\right|^2 + 1}, \tag{11}$$

$$\gamma'^{x_1'}_{e2} = \rho_{u_1}\left|h_{u_1 e}\right|^2. \tag{12}$$

In the third time slot, it can be seen from (4) that user u_1 knows the data sent by itself and its own associated CSI, so the first term in (4) is recognized as a self-interference term. Here it is assumed that the self-interference terms can

be canceled completely at u_1. Thus, the signal received by u_1 can be further rewritten as

$$y_{r\to u_1} = \sqrt{P_{u_2}}\beta h_{ru_1}h_{ru_2}x_2' + \beta h_{ru_1}n_r + n_{u_1}. \tag{13}$$

From (13), we know that the SNR of u_1 decoding x_2' is

$$\gamma_{u_2\to r\to u_1} = \frac{\rho_{u_2}\rho_r\left|h_{ru_1}\right|^2\left|h_{ru_2}\right|^2}{\left(\rho_r+\rho_{u_1}\right)\left|h_{ru_1}\right|^2+\rho_{u_2}\left|h_{ru_2}\right|^2+1}. \tag{14}$$

After x_2' is successfully decoded, x_2' is demodulated and converted into binary bitstream data s_2'. Then, we employ bit-level XOR processing to obtain $s_2'\oplus s_p = s_2\oplus s_p\oplus s_p = s_2$, so that the data s_2 sent by u_2 can be obtained. Similarly, the SNR of u_2 decoding x_1' can be obtained from (4) as

$$\gamma_{u_1\to r\to u_2} = \frac{\rho_{u_1}\rho_r\left|h_{ru_1}\right|^2\left|h_{ru_2}\right|^2}{\left(\rho_r+\rho_{u_2}\right)\left|h_{ru_2}\right|^2+\rho_{u_1}\left|h_{ru_1}\right|^2+1}. \tag{15}$$

Using a similar operation as u_1, u_2 can get the data s_1 sent by user u_1.

For the eavesdropper e, the decoding situation can be divided into the following four cases as follows:

Case 1: If x_1' and x_2' have been decoded successfully in the second time slot, e does not do any processing of the received data in the third time slot.

Case 2: Only the data x_1' is successfully decoded in the second time slot and the eavesdropper e eliminates the term containing x_1' from the received AF signal, so that (4) can be rewritten as

$$y_{r\to e} = \sqrt{P_{u_2}}\beta h_{u_2r}h_{re}x_2' + \beta h_{re}n_r + n_e. \tag{16}$$

From (16), we can obtain the SNR of e decoding x_2' as

$$\gamma_{e3,2}^{x_2'} = \frac{\rho_{u_2}\rho_r\left|h_{u_2r}\right|^2|h_{re}|^2}{\rho_r|h_{re}|^2+\rho_{u_2}\left|h_{u_2r}\right|^2+\rho_{u_1}\left|h_{u_1r}\right|^2+1}. \tag{17}$$

Case 3: Only the data x_2' is successfully decoded in the second time slot, similarly, (4) can be rewritten as

$$y_{r\to e} = \sqrt{P_{u_1}}\beta h_{u_1r}h_{re}x_1' + \beta h_{re}n_r + n_e. \tag{18}$$

Thus, the SNR of e decoding x_1' can be obtained as

$$\gamma_{e3,3}^{x_1'} = \frac{\rho_{u_1}\rho_r\left|h_{u_1r}\right|^2|h_{re}|^2}{\rho_r|h_{re}|^2+\rho_{u_1}\left|h_{u_1r}\right|^2+\rho_{u_2}\left|h_{u_2r}\right|^2+1}. \tag{19}$$

Case 4: If both x_1' and x_2' cannot be decoded successfully in the second time slot, e can use the signal received in the third time slot to decode x_1' and x_2'. The decoding order is divided into two cases:

① The eavesdropper e decodes the signals in the order of $x_1'\to x_2'$, thus the corresponding SNRs are respectively as (20), shown at the bottom of the next page, and (21).

$$\gamma_{e3,4}^{x_2'} = \frac{\rho_{u_2}\rho_r\left|h_{u_2r}\right|^2|h_{re}|^2}{\rho_r|h_{re}|^2+\rho_{u_1}\left|h_{u_1r}\right|^2+\rho_{u_2}\left|h_{u_2r}\right|^2+1}. \tag{21}$$

② The eavesdropper e decodes the signals in the order of $x_2'\to x_1'$, thus the corresponding SNRs are respectively as (22), shown at the bottom of the next page, and (23).

$$\gamma_{e3,4}^{\prime x_1'} = \frac{\rho_{u_1}\rho_r\left|h_{u_1r}\right|^2|h_{re}|^2}{\rho_r|h_{re}|^2+\rho_{u_1}\left|h_{u_1r}\right|^2+\rho_{u_2}\left|h_{u_2r}\right|^2+1}. \tag{23}$$

III. PERFORMANCE ANALYSIS

In this section, outage probability and intercept probability for the proposed transmission protocol are investigated in this system. Normally, the communication between two points is considered to be outage when the SNR of the data transmitted between them falls below the preset SNR transmission threshold T, otherwise it will be considered to be successful transmission, i.e., successfully intercepted.

A. OUTAGE PERFORMANCE ANALYSIS

To achieve secure and successful data exchange between two users in this system, all SNR equations (8), (14) and (15) must be greater than T. Therefore, the outage probability of the system can be expressed as

$$P_{out} = 1-\Pr\left\{\begin{array}{l}\gamma_{u_1}^{x_s}>T,\gamma_{u_2}^{x_s}>T,\\ \min\left\{\gamma_{u_2\to r\to u_1},\gamma_{u_1\to r\to u_2}\right\}>T\end{array}\right\}. \tag{24}$$

According to the literature [35], the tight upper bounds of $\gamma_{u_2\to r\to u_1}$ and $\gamma_{u_1\to r\to u_2}$ are known to be

$$\gamma_{u_2\to r\to u_1} \le \rho_r\min\left\{\frac{P_{u_2}}{P_r+P_{u_1}}\left|h_{ru_2}\right|^2,\left|h_{ru_1}\right|^2\right\}, \tag{25}$$

$$\gamma_{u_1\to r\to u_2} < \rho_r\min\left\{\frac{P_{u_1}}{P_r+P_{u_2}}\left|h_{ru_1}\right|^2,\left|h_{ru_2}\right|^2\right\} \tag{26}$$

$\gamma_{u_2\to r\to u_1}$ and $\gamma_{u_1\to r\to u_2}$ in (24) are replaced with the tight upper bounds, the tight lower bound of the outage probability of the system can be obtained as

$$\begin{aligned}P_{out} &\ge 1-\Pr\left\{\begin{array}{l}\left|h_{su_1}\right|^2>\frac{T}{\rho_s},\left|h_{su_2}\right|^2>\frac{T}{\rho_s},\\ \min\left\{\frac{P_{u_1}}{P_r+P_{u_2}},1\right\}\left|h_{ru_1}\right|^2>\frac{T}{\rho_r},\\ \min\left\{\frac{P_{u_2}}{P_r+P_{u_1}},1\right\}\left|h_{ru_2}\right|^2>\frac{T}{\rho_r}\end{array}\right\}\\ &= 1-e^{-\frac{T\left(\sigma_{su_1}^2+\sigma_{su_2}^2\right)}{\rho_s\sigma_{su_1}^2\sigma_{su_2}^2}}\left(I_1+I_2\right),\end{aligned} \tag{27}$$

where

$$\begin{aligned}I_1 &= \Pr\left\{\begin{array}{l}P_s|h_{sr}|^2>P_{th},\\ \min\left\{\frac{\theta P_{u_1}}{2\eta P_{th}+\theta P_{u_2}},1\right\}\left|h_{ru_1}\right|^2>\frac{\theta T}{2\eta\rho_{th}},\\ \min\left\{\frac{\theta P_{u_2}}{2\eta P_{th}+\theta P_{u_1}},1\right\}\left|h_{ru_2}\right|^2>\frac{\theta T}{2\eta\rho_{th}}\end{array}\right\}\\ &= \exp\left(\begin{array}{l}-\frac{P_{th}}{P_s\sigma_{sr}^2}-\frac{\theta T}{2\eta\rho_{th}\sigma_{ru_1}^2}\max\left\{\frac{2\eta P_{th}+\theta P_{u_2}}{\theta P_{u_1}},1\right\}\\ -\frac{\theta T}{2\eta\rho_{th}\sigma_{ru_2}^2}\max\left\{\frac{2\eta P_{th}+\theta P_{u_1}}{\theta P_{u_2}},1\right\}\end{array}\right),\end{aligned} \tag{28}$$

$\theta = (1-\alpha)/\alpha$.

$$I_2 = \Pr\left\{\begin{array}{l} P_{\min} < P_s|h_{sr}|^2 \le P_{th}, \\ \min\left\{\frac{\theta P_{u_1}}{2\eta P_s|h_{sr}|^2+\theta P_{u_2}}, 1\right\}|h_{sr}|^2\left|h_{ru_1}\right|^2 > \frac{\theta T}{2\eta\rho_s}, \\ \min\left\{\frac{\theta P_{u_2}}{2\eta P_s|h_{sr}|^2+\theta P_{u_1}}, 1\right\}|h_{sr}|^2\left|h_{ru_2}\right|^2 > \frac{\theta T}{2\eta\rho_s} \end{array}\right\}. \tag{29}$$

Case 1: When $P_{u_1} > P_{u_2}$,

$$\begin{aligned} I_2 &= \Pr\left\{\begin{array}{l} P_{\min} < P_s|h_{sr}|^2 \le P_{th}, \\ \frac{2\eta P_s|h_{sr}|^2}{\theta} < P_{u_1} - P_{u_2}, \\ \frac{2\eta\rho_s|h_{sr}|^2\left|h_{ru_1}\right|^2}{\theta} > T, \\ \frac{2\eta P_s|h_{sr}|^2\left|h_{ru_2}\right|^2}{2\eta P_s|h_{sr}|^2+\theta P_{u_1}}\rho_{u_2} > T \end{array}\right\} \\ &+ \Pr\left\{\begin{array}{l} P_{\min} < P_s|h_{sr}|^2 \le P_{th}, \\ \frac{2\eta P_s|h_{sr}|^2}{\theta} > P_{u_1} - P_{u_2}, \\ \frac{2\eta P_s|h_{sr}|^2\rho_{u_1}\left|h_{ru_1}\right|^2}{2\eta P_s|h_{sr}|^2+\theta P_{u_2}} > T, \\ \frac{2\eta P_s|h_{sr}|^2\rho_{u_2}\left|h_{ru_2}\right|^2}{2\eta P_s|h_{sr}|^2+\theta P_{u_1}} > T \end{array}\right\} \\ &= \Pr\left\{\begin{array}{l} \frac{P_{\min}}{P_s} < |h_{sr}|^2 \le \frac{P_{th}}{P_s}, \\ |h_{sr}|^2 < \frac{\theta(P_{u_1}-P_{u_2})}{2\eta P_s}, \\ \left|h_{ru_1}\right|^2 > \frac{\theta T}{2\eta\rho_s|h_{sr}|^2}, \\ \left|h_{ru_2}\right|^2 > \frac{T(2\eta P_s|h_{sr}|^2+\theta P_{u_1})}{2\eta\rho_{u_2}P_s|h_{sr}|^2} \end{array}\right\} \\ &+ \Pr\left\{\begin{array}{l} \frac{P_{\min}}{P_s} < |h_{sr}|^2 \le P_s, \\ \left|h_{ru_1}\right|^2 > \frac{T(2\eta P_s|h_{sr}|^2+\theta P_{u_2})}{2\eta\rho_{u_1}P_s|h_{sr}|^2}, \\ |h_{sr}|^2 > \frac{\theta(P_{u_1}-P_{u_2})}{2\eta P_s}, \\ \left|h_{ru_2}\right|^2 > \frac{T(2\eta P_s|h_{sr}|^2+\theta P_{u_1})}{2\eta\rho_{u_2}P_s|h_{sr}|^2} \end{array}\right\}. \end{aligned} \tag{30}$$

In the case of $\theta\left(P_{u_1} - P_{u_2}\right) < 2\eta P_{\min}$,

$$\begin{aligned} I_2 &= \Pr\left\{\begin{array}{l} \frac{P_{\min}}{P_s} < |h_{sr}|^2 \le \frac{P_{th}}{P_s}, \\ \left|h_{ru_2}\right|^2 > \frac{T(2\eta P_s|h_{sr}|^2+\theta P_{u_1})}{2\eta\rho_{u_2}P_s|h_{sr}|^2}, \\ \left|h_{ru_1}\right|^2 > \frac{T(2\eta P_s|h_{sr}|^2+\theta P_{u_2})}{2\eta\rho_{u_1}P_s|h_{sr}|^2} \end{array}\right\} \\ &= \frac{1}{\sigma_{sr}^2}e^{-\frac{T}{\rho_{u_1}\sigma_{ru_1}^2}-\frac{T}{\rho_{u_2}\sigma_{ru_2}^2}} \\ &\times \int_{\frac{P_{\min}}{P_s}}^{\frac{P_{th}}{P_s}} e^{-\frac{x}{\sigma_{sr}^2}-\left(\frac{P_{u_2}}{P_{u_1}\sigma_{ru_1}^2}+\frac{P_{u_1}}{P_{u_2}\sigma_{ru_2}^2}\right)\frac{\theta T}{2\eta\rho_s x}}dx \\ &= \frac{1}{\sigma_{sr}^2}e^{-\frac{T\left(\rho_{u_1}\sigma_{ru_1}^2+\rho_{u_2}\sigma_{ru_2}^2\right)}{\rho_{u_1}\sigma_{ru_1}^2\rho_{u_2}\sigma_{ru_2}^2}} \\ &\times Q\left(\frac{P_{\min}}{P_s}, \frac{P_{th}}{P_s}, \frac{1}{\sigma_{sr}^2}, \left(\frac{P_{u_2}}{P_{u_1}\sigma_{ru_1}^2}+\frac{P_{u_1}}{P_{u_2}\sigma_{ru_2}^2}\right)\frac{\theta T}{2\eta\rho_s}\right), \end{aligned} \tag{31}$$

where $Q(x_0, x_1, a, b) \approx \left(e^{-ax_0} - e^{-ax_1}\right)\sqrt{4b/a}K_1\left(\sqrt{4ab}\right)$ is the modified Bessel function of the second kind.

In the case of $2\eta P_{\min} < \theta\left(P_{u_1} - P_{u_2}\right) \le 2\eta P_{th}$, the closed-form result of I_2 is shown in (32), at the bottom of the next page.

In the case of $\theta\left(P_{u_1} - P_{u_2}\right) > 2\eta P_{th}$,

$$\begin{aligned} &I_2 \\ &= \Pr\left\{\begin{array}{l} \frac{P_{\min}}{P_s} < |h_{sr}|^2 \le \frac{P_{th}}{P_s}, \left|h_{ru_1}\right|^2 > \frac{\theta T}{2\eta\rho_s|h_{sr}|^2}, \\ \left|h_{ru_2}\right|^2 > \frac{T(2\eta P_s|h_{sr}|^2+\theta P_{u_1})}{2\eta\rho_{u_2}P_s|h_{sr}|^2} \end{array}\right\} \\ &= \frac{1}{\sigma_{sr}^2}e^{-\frac{T}{\rho_{u_2}\sigma_{ru_2}^2}}\int_{\frac{P_{\min}}{P_s}}^{\frac{P_{th}}{P_s}} e^{-\frac{x}{\sigma_{sr}^2}-\left(\frac{1}{\sigma_{ru_1}^2}+\frac{P_{u_1}}{P_{u_2}\sigma_{ru_2}^2}\right)\frac{\theta T}{2\eta\rho_s x}}dx \\ &= \frac{1}{\sigma_{sr}^2}e^{-\frac{T}{\rho_{u_2}\sigma_{ru_2}^2}}Q\left(\frac{P_{\min}}{P_s}, \frac{P_{th}}{P_s}, \frac{1}{\sigma_{sr}^2}, \left(\frac{1}{\sigma_{ru_1}^2}+\frac{P_{u_1}}{P_{u_2}\sigma_{ru_2}^2}\right)\frac{\theta T}{2\eta\rho_s}\right). \end{aligned} \tag{33}$$

Case 2: When $P_{u_1} < P_{u_2}$,

$$\begin{aligned} I_2 &= \Pr\left\{\begin{array}{l} P_{\min} < P_s|h_{sr}|^2 \le P_{th}, \\ \frac{2\eta P_s|h_{sr}|^2}{\theta} < P_{u_2} - P_{u_1}, \\ \frac{2\eta P_s|h_{sr}|^2\left|h_{ru_1}\right|^2}{2\eta P_s|h_{sr}|^2+\theta P_{u_2}}\rho_{u_1} > T, \\ \frac{2\eta\rho_s|h_{sr}|^2\left|h_{ru_2}\right|^2}{\theta} > T \end{array}\right\} \\ &+ \Pr\left\{\begin{array}{l} P_{\min} < P_s|h_{sr}|^2 \le P_{th}, \\ \frac{2\eta P_s|h_{sr}|^2}{\theta} > P_{u_2} - P_{u_1}, \\ \frac{2\eta P_s|h_{sr}|^2\left|h_{ru_1}\right|^2}{2\eta P_s|h_{sr}|^2+\theta P_{u_2}}\rho_{u_1} > T, \\ \frac{2\eta P_s|h_{sr}|^2\left|h_{ru_2}\right|^2}{2\eta P_s|h_{sr}|^2+\theta P_{u_1}}\rho_{u_2} > T \end{array}\right\} \end{aligned}$$

$$\gamma_{e3,4}^{x_1'} = \frac{\rho_{u_1}\rho_r\left|h_{u_1r}\right|^2|h_{re}|^2}{\rho_{u_2}\rho_r\left|h_{u_2r}\right|^2|h_{re}|^2 + \rho_r|h_{re}|^2 + \rho_{u_1}\left|h_{u_1r}\right|^2 + \rho_{u_2}\left|h_{u_2r}\right|^2 + 1} \tag{20}$$

$$\gamma_{e3,4}^{x_2'} = \frac{\rho_{u_2}\rho_r\left|h_{u_2r}\right|^2|h_{re}|^2}{\rho_{u_1}\rho_r\left|h_{u_1r}\right|^2|h_{re}|^2 + \rho_r|h_{re}|^2 + \rho_{u_1}\left|h_{u_1r}\right|^2 + \rho_{u_2}\left|h_{u_2r}\right|^2 + 1} \tag{22}$$

$$= \Pr\left\{\begin{array}{l}\frac{P_{\min}}{P_s} < |h_{sr}|^2 \le \frac{P_{th}}{P_s},\\ |h_{sr}|^2 < \frac{\theta\left(P_{u_2}-P_{u_1}\right)}{2\eta P_s},\\ \left|h_{ru_1}\right|^2 > \frac{T\left(2\eta P_s|h_{sr}|^2+\theta P_{u_2}\right)}{2\eta\rho_{u_1}P_s|h_{sr}|^2},\\ \left|h_{ru_2}\right|^2 > \frac{\theta T}{2\eta\rho_s|h_{sr}|^2}\end{array}\right\}$$
$$+ \Pr\left\{\begin{array}{l}\frac{P_{\min}}{P_s} < |h_{sr}|^2 \le \frac{P_{th}}{P_s},\\ \left|h_{ru_1}\right|^2 > \frac{T\left(2\eta P_s|h_{sr}|^2+\theta P_{u_2}\right)}{2\eta\rho_{u_1}P_s|h_{sr}|^2},\\ |h_{sr}|^2 > \frac{\theta\left(P_{u_2}-P_{u_1}\right)}{2\eta P_s},\\ \left|h_{ru_2}\right|^2 > \frac{T\left(2\eta P_s|h_{sr}|^2+\theta P_{u_1}\right)}{2\eta\rho_{u_2}P_s|h_{sr}|^2}\end{array}\right\}. \quad (34)$$

In the case of $\theta\left(P_{u_2}-P_{u_1}\right) < 2\eta P_{\min}$,

$$I_2 = \Pr\left\{\begin{array}{l}\frac{P_{\min}}{P_s} < |h_{sr}|^2 \le \frac{P_{th}}{P_s},\\ \left|h_{ru_2}\right|^2 > \frac{T\left(2\eta P_s|h_{sr}|^2+\theta P_{u_1}\right)}{2\eta\rho_{u_2}P_s|h_{sr}|^2},\\ \left|h_{ru_1}\right|^2 > \frac{T\left(2\eta P_s|h_{sr}|^2+\theta P_{u_2}\right)}{2\eta\rho_{u_1}P_s|h_{sr}|^2}\end{array}\right\}$$
$$= \frac{1}{\sigma_{sr}^2} e^{-\frac{T}{\rho_{u_1}\sigma_{ru_1}^2}-\frac{T}{\rho_{u_2}\sigma_{ru_2}^2}} \times \int_{\frac{P_{\min}}{P_s}}^{\frac{P_{th}}{P_s}} e^{-\frac{x}{\sigma_{sr}^2}-\left(\frac{P_{u_2}}{P_{u_1}\sigma_{ru_1}^2}+\frac{P_{u_1}}{P_{u_2}\sigma_{ru_2}^2}\right)\frac{\theta T}{2\eta\rho_s x}} dx$$
$$= \frac{1}{\sigma_{sr}^2} e^{-\frac{T}{\rho_{u_1}\sigma_{ru_1}^2}-\frac{T}{\rho_{u_2}\sigma_{ru_2}^2}} \times Q\left(\frac{P_{\min}}{P_s}, \frac{P_{th}}{P_s}, \frac{1}{\sigma_{sr}^2}, \left(\frac{P_{u_2}}{P_{u_1}\sigma_{ru_1}^2}+\frac{P_{u_1}}{P_{u_2}\sigma_{ru_2}^2}\right)\frac{\theta T}{2\eta\rho_s}\right). \quad (35)$$

In the case of $2\eta P_{\min} < \theta\left(P_{u_2}-P_{u_1}\right) \le 2\eta P_{th}$, the closed-form result of I_2 is shown in (36), at the bottom of the next page.

In the case of $2\eta P_{th} < \theta\left(P_{u_2}-P_{u_1}\right)$,

I_2

$$= \Pr\left\{\begin{array}{l}\frac{P_{\min}}{P_s} < |h_{sr}|^2 \le \frac{P_{th}}{P_s}, \left|h_{ru_2}\right|^2 > \frac{\theta T}{2\eta\rho_s|h_{sr}|^2},\\ \left|h_{ru_1}\right|^2 > \frac{T\left(2\eta P_s|h_{sr}|^2+\theta P_{u_2}\right)}{2\eta\rho_{u_1}P_s|h_{pr}|^2}\end{array}\right\}$$
$$= \frac{1}{\sigma_{sr}^2} e^{-\frac{T}{\rho_{u_1}\sigma_{ru_1}^2}} \int_{\frac{P_{\min}}{P_s}}^{\frac{P_{th}}{P_s}} e^{-\frac{x}{\sigma_{sr}^2}-\left(\frac{P_{u_2}}{P_{u_1}\sigma_{ru_1}^2}+\frac{1}{\sigma_{ru_2}^2}\right)\frac{\theta T}{2\eta\rho_s x}} dx$$
$$= \frac{1}{\sigma_{sr}^2} e^{-\frac{T}{\rho_{u_1}\sigma_{ru_1}^2}} Q\left(\frac{P_{\min}}{P_s}, \frac{P_{th}}{P_s}, \frac{1}{\sigma_{sr}^2}, \left(\frac{P_{u_2}}{P_{u_1}\sigma_{ru_1}^2}+\frac{1}{\sigma_{ru_2}^2}\right)\frac{\theta T}{2\eta\rho_s}\right). \quad (37)$$

Finally, by substituting (28)-(37) into (27), we can get the closed-form tight lower bound of outage probability of the considered system with the proposed forward protocol.

B. INTERCEPT PERFORMANCE ANALYSIS

Due to the fact that there is no direct communication link between s and e in this model, the eavesdropper e can never intercept the data s_s sent by s. Moreover, the signals transmitted by these two users are made bit-level XOR with s_s, so the eavesdropper e will never be able to successfully decode data exchanged between u_1 and u_2.

In order to be able to show the intercept probability of eavesdropper e in the simulation diagram, it is assumed that e is able to receive the weak signal sent by s. Then the signal received by e in the first time slot is shown in (1) in the case of $\tau = e$, and the SNR of e decoding x_s is $\gamma_e^{x_s} = \rho_s|h_{se}|^2$, where the variance of h_{se} satisfies $\sigma_{se}^2 \ll 1$. The probability of e successfully decoding x_s is

$$P_{succ}^I = \Pr\left\{\gamma_e^{x_s} > T\right\} = e^{-\frac{T}{\rho_s\sigma_{se}^2}}. \quad (38)$$

According to (9), (10), (11) and (12), we know the probability of e successfully decoding x_1' and x_2' in the second time slot can be derived as (39), shown at the bottom of the next page.

In the third time slot, the intercept probability of decoding x_1' and x_2' can be calculated in three cases as follows:

$$I_2 = \Pr\left\{\frac{P_{\min}}{P_s} < |h_{sr}|^2 \le \frac{\theta\left(P_{u_1}-P_{u_2}\right)}{2\eta P_s}, \left|h_{ru_1}\right|^2 > \frac{\theta T}{2\eta\rho_s|h_{sr}|^2}, \left|h_{ru_2}\right|^2 > \frac{T\left(2\eta P_s|h_{sr}|^2+\theta P_{u_1}\right)}{2\eta\rho_{u_2}P_s|h_{sr}|^2}\right\}$$
$$+ \Pr\left\{\frac{\theta\left(P_{u_1}-P_{u_2}\right)}{2\eta P_s} < |h_{sr}|^2 \le \frac{P_{th}}{P_s}, \left|h_{ru_1}\right|^2 > \frac{T\left(2\eta P_s|h_{sr}|^2+\theta P_{u_2}\right)}{2\eta\rho_{u_1}P_s|h_{sr}|^2}, \left|h_{ru_2}\right|^2 > \frac{T\left(2\eta P_s|h_{sr}|^2+\theta P_{u_1}\right)}{2\eta\rho_{u_2}P_s|h_{sr}|^2}\right\}$$
$$= \frac{1}{\sigma_{sr}^2} e^{-\frac{T}{\rho_{u_2}\sigma_{ru_2}^2}} \int_{\frac{P_{\min}}{P_s}}^{\frac{\theta\left(P_{u_1}-P_{u_2}\right)}{2\eta P_s}} e^{-\frac{x}{\sigma_{sr}^2}-\left(\frac{1}{\sigma_{ru_1}^2}+\frac{P_{u_1}}{P_{u_2}\sigma_{ru_2}^2}\right)\frac{\theta T}{2\eta\rho_s x}} dx + \frac{1}{\sigma_{sr}^2} e^{-\left(\frac{T}{\rho_{u_1}\sigma_{ru_1}^2}+\frac{T}{\rho_{u_2}\sigma_{ru_2}^2}\right)} \int_{\frac{\theta\left(P_{u_1}-P_{u_2}\right)}{2\eta P_s}}^{\frac{P_{th}}{P_s}} e^{-\frac{x}{\sigma_{sr}^2}-\left(\frac{P_{u_2}}{P_{u_1}\sigma_{ru_1}^2}+\frac{P_{u_1}}{P_{u_2}\sigma_{ru_2}^2}\right)\frac{\theta T}{2\eta\rho_s x}} dx$$
$$= \frac{1}{\sigma_{sr}^2} e^{-\frac{T}{\rho_{u_2}\sigma_{ru_2}^2}} Q\left(\frac{P_{\min}}{P_s}, \frac{\theta\left(P_{u_1}-P_{u_2}\right)}{2\eta P_s}, \frac{1}{\sigma_{sr}^2}, \left(\frac{1}{\sigma_{ru_1}^2}+\frac{P_{u_1}}{P_{u_2}\sigma_{ru_2}^2}\right)\frac{\theta T}{2\eta\rho_s}\right)$$
$$+ \frac{1}{\sigma_{sr}^2} e^{-\left(\frac{T}{\rho_{u_1}\sigma_{ru_1}^2}+\frac{T}{\rho_{u_2}\sigma_{ru_2}^2}\right)} Q\left(\frac{\theta\left(P_{u_1}-P_{u_2}\right)}{2\eta P_s}, \frac{P_{th}}{P_s}, \frac{1}{\sigma_{sr}^2}, \left(\frac{P_{u_2}}{P_{u_1}\sigma_{ru_1}^2}+\frac{P_{u_1}}{P_{u_2}\sigma_{ru_2}^2}\right)\frac{\theta T}{2\eta\rho_s}\right) \quad (32)$$

1) When only x_1' is decoded successfully in the second time slot, x_2' is need to be decoded by e in the third time slot. In this case, the probability of successfully decoding x_1' and x_2' can be denoted by

$$P_{succ}^{I-x_1',II-x_2'} = \Pr\left\{\gamma_{e2}^{x_1'} > T, \gamma_{e2}^{x_2'} < T, \gamma_{e3,2}^{x_2'} > T\right\}. \quad (40)$$

The SNR of e decoding x_2' in (17) can approximately satisfy the following relation

$$\begin{aligned}\frac{1}{\gamma_{e3,2}^{x_2'}} &\approx \frac{1}{\rho_{u_2}\left|h_{u_2r}\right|^2} + \frac{1}{\rho_r|h_{re}|^2} + \frac{\rho_{u_1}\left|h_{u_1r}\right|^2}{\rho_{u_2}\rho_r\left|h_{u_2r}\right|^2|h_{re}|^2} \\ &\geq \max\left\{\frac{1}{\rho_{u_2}\left|h_{u_2r}\right|^2}, \frac{1}{\rho_r|h_{re}|^2}, \frac{\rho_{u_1}\left|h_{u_1r}\right|^2}{\rho_{u_2}\rho_r\left|h_{u_2r}\right|^2|h_{re}|^2}\right\}.\end{aligned} \quad (41)$$

From (41), we can obtain the tight upper bound of $\gamma_{e3,2}^{x_2'}$ as follows:

$$\gamma_{e3,2}^{x_2'} \leq \min\left\{\rho_{u_2}\left|h_{u_2r}\right|^2, \rho_r|h_{re}|^2, \frac{\rho_{u_2}\rho_r\left|h_{u_2r}\right|^2|h_{re}|^2}{\rho_{u_1}\left|h_{u_1r}\right|^2}\right\}. \quad (42)$$

$\gamma_{e3,2}^{x_2'}$ in (24) are replaced with (42), the tight upper bound of (40) can be obtained as

$$\begin{aligned}P_{succ}^{I-x_1',II-x_2'} &\leq \Pr\left\{\frac{\rho_{u_1}\left|h_{u_1e}\right|^2}{\rho_{u_2}\left|h_{u_2e}\right|^2+1} > T, \rho_{u_2}\left|h_{u_2e}\right|^2 < T\right\} \\ &\times \Pr\left\{\min\left\{\rho_{u_2}\left|h_{u_2r}\right|^2, \rho_r|h_{re}|^2, \frac{\rho_{u_2}\rho_r\left|h_{u_2r}\right|^2|h_{re}|^2}{\rho_{u_1}\left|h_{u_1r}\right|^2}\right\} > T\right\} \\ &= g_1\left(A_1+B_1\right), \end{aligned} \quad (43)$$

where g_1, A_1 and B_1 are shown in (44), (45) and (46), in which (45) and (46) are shown at the bottom of the next page, $E_1(x) = \int_x^{+\infty}\frac{1}{t}e^{-t}dt$.

$$\begin{aligned}g_1 &= \Pr\left\{\frac{\rho_{u_1}\left|h_{u_1e}\right|^2}{\rho_{u_2}\left|h_{u_2e}\right|^2+1} > T, \rho_{u_2}\left|h_{u_2e}\right|^2 < T\right\} \\ &= \frac{\rho_{u_1}\sigma_{u_1e}^2}{\rho_{u_1}\sigma_{u_1e}^2 + T\rho_{u_2}\sigma_{u_2e}^2}\left(1 - e^{-\frac{\rho_{u_1}\sigma_{u_1e}^2+T\rho_{u_2}\sigma_{u_2e}^2}{\rho_{u_1}\sigma_{u_1e}^2\sigma_{u_2e}^2}\frac{T}{\rho_{u_2}}}\right) \\ &\quad e^{-\frac{T}{\rho_{u_1}\sigma_{u_1e}^2}}, \end{aligned} \quad (44)$$

2) When only x_2' is decoded successfully in the second time slot, x_1' is need to be decoded by e in the third time slot. In this case, the probability of successfully decoding x_1' and x_2' can be denoted by

$$P_{succ}^{I-x_1',II-x_2'} = \Pr\left\{\gamma'^{x_2'}_{e2} > T, \gamma'^{x_1'}_{e2} < T, \gamma'^{x_1'}_{e3,3} > T\right\}. \quad (47)$$

$$\begin{aligned}I_2 &= \Pr\left\{\frac{P_{\min}}{P_s} < |h_{sr}|^2 < \frac{\theta\left(P_{u_2}-P_{u_1}\right)}{2\eta P_s}, \left|h_{ru_1}\right|^2 > \frac{T\left(2\eta P_s|h_{sr}|^2+\theta P_{u_2}\right)}{2\eta\rho_{u_1}P_s|h_{sr}|^2}, \left|h_{ru_2}\right|^2 > \frac{\theta T}{2\eta\rho_s|h_{sr}|^2}\right\} \\ &\quad + \Pr\left\{\frac{\theta\left(P_{u_2}-P_{u_1}\right)}{2\eta P_s} < |h_{sr}|^2 \leq \frac{P_{th}}{P_s}, \left|h_{ru_1}\right|^2 > \frac{T\left(2\eta P_s|h_{sr}|^2+\theta P_{u_2}\right)}{2\eta\rho_{u_1}P_s|h_{sr}|^2}, \left|h_{ru_2}\right|^2 > \frac{T\left(2\eta P_s|h_{sr}|^2+\theta P_{u_1}\right)}{2\eta\rho_{u_2}P_s|h_{sr}|^2}\right\} \\ &= \frac{1}{\sigma_{sr}^2}e^{-\frac{T}{\rho_{u_1}\sigma_{ru_1}^2}}\int_{\frac{P_{\min}}{P_s}}^{\frac{\theta\left(P_{u_2}-P_{u_1}\right)}{2\eta P_s}} e^{-\frac{x}{\sigma_{sr}^2}-\left(\frac{P_{u_2}}{P_{u_1}\sigma_{ru_1}^2}+\frac{1}{\sigma_{ru_2}^2}\right)\frac{\theta T}{2\eta\rho_s x}}dx + \frac{1}{\sigma_{sr}^2}e^{-\left(\frac{T}{\rho_{u_1}\sigma_{ru_1}^2}+\frac{T}{\rho_{u_2}\sigma_{ru_2}^2}\right)}\int_{\frac{\theta\left(P_{u_2}-P_{u_1}\right)}{2\eta P_s}}^{\frac{P_{th}}{P_s}} e^{-\frac{x}{\sigma_{sr}^2}-\left(\frac{P_{u_2}}{P_{u_1}\sigma_{ru_1}^2}+\frac{P_{u_1}}{P_{u_2}\sigma_{ru_2}^2}\right)\frac{\theta T}{2\eta\rho_s x}}dx \\ &= \frac{1}{\sigma_{sr}^2}e^{-\frac{T}{\rho_{u_1}\sigma_{ru_1}^2}}Q\left(\frac{P_{\min}}{P_s}, \frac{\theta\left(P_{u_2}-P_{u_1}\right)}{2\eta P_s}, \frac{1}{\sigma_{sr}^2}, \left(\frac{P_{u_2}}{P_{u_1}\sigma_{ru_1}^2}+\frac{1}{\sigma_{ru_2}^2}\right)\frac{\theta T}{2\eta\rho_s}\right) \\ &\quad + \frac{1}{\sigma_{sr}^2}e^{-\left(\frac{T}{\rho_{u_1}\sigma_{ru_1}^2}+\frac{T}{\rho_{u_2}\sigma_{ru_2}^2}\right)}Q\left(\frac{\theta\left(P_{u_2}-P_{u_1}\right)}{2\eta P_s}, \frac{P_{th}}{P_s}, \frac{1}{\sigma_{sr}^2}, \left(\frac{P_{u_2}}{P_{u_1}\sigma_{ru_1}^2}+\frac{P_{u_1}}{P_{u_2}\sigma_{ru_2}^2}\right)\frac{\theta T}{2\eta\rho_s}\right) \end{aligned} \quad (36)$$

$$\begin{aligned}P_{succ}^{II} &= \Pr\left\{\frac{\rho_{u_1}\left|h_{u_1e}\right|^2}{\rho_{u_2}\left|h_{u_2e}\right|^2+1} > T, \rho_{u_2}\left|h_{u_2e}\right|^2 > T\right\} + \Pr\left\{\frac{\rho_{u_2}\left|h_{u_2e}\right|^2}{\rho_{u_1}\left|h_{u_1e}\right|^2+1} > T, \rho_{u_1}\left|h_{u_1e}\right|^2 > T\right\} \\ &= \int_{\frac{T}{\rho_{u_2}}}^{+\infty} f_{\left|h_{u_2e}\right|^2}(x)\Pr\left\{\left|h_{u_1e}\right|^2 > \frac{T\rho_{u_2}x+T}{\rho_{u_1}}\right\}dx + \int_{\frac{T}{\rho_{u_1}}}^{+\infty} f_{\left|h_{u_1e}\right|^2}(x)\Pr\left\{\left|h_{u_2e}\right|^2 > \frac{T\rho_{u_1}x+T}{\rho_{u_2}}\right\}dx \\ &= \frac{P_{u_1}\sigma_{u_1e}^2}{P_{u_1}\sigma_{u_1e}^2+TP_{u_2}\sigma_{u_2e}^2}e^{-\frac{T}{\rho_{u_1}\sigma_{u_1e}^2}-\frac{P_{u_1}\sigma_{u_1e}^2+TP_{u_2}\sigma_{u_2e}^2}{P_{u_1}\sigma_{u_1e}^2\sigma_{u_2e}^2}\frac{T}{\rho_{u_2}}}+\frac{P_{u_2}\sigma_{u_2e}^2}{P_{u_2}\sigma_{u_2e}^2+TP_{u_1}\sigma_{u_1e}^2}e^{-\frac{T}{\rho_{u_2}\sigma_{u_2e}^2}-\frac{P_{u_2}\sigma_{u_2e}^2+TP_{u_1}\sigma_{u_1e}^2}{\sigma_{u_1e}^2P_{u_2}\sigma_{u_2e}^2}\frac{T}{\rho_{u_1}}}} \end{aligned} \quad (39)$$

Similarly, the tight upper bound of $\gamma_{e3,3}^{x_1'}$ is

$$\gamma_{e3,3}^{x_1'} \le \min\left\{\rho_{u_1}\left|h_{u_1r}\right|^2, \rho_r|h_{re}|^2, \frac{\rho_{u_1}\rho_r\left|h_{u_1r}\right|^2|h_{re}|^2}{\rho_{u_2}\left|h_{u_2r}\right|^2}\right\}. \tag{48}$$

Therefore, the tight upper bound of (47) can be obtained as

$$\begin{aligned} &P_{succ}^{I-x_2',II-x_1'} \\ &\le \Pr\left\{\frac{\rho_{u_2}\left|h_{u_2e}\right|^2}{\rho_{u_1}\left|h_{u_1e}\right|^2+1} > T, \rho_{u_1}\left|h_{u_1e}\right|^2 < T\right\} \\ &\times \Pr\left\{\min\left\{\rho_{u_1}\left|h_{u_1r}\right|^2, \rho_r|h_{re}|^2, \frac{\rho_{u_1}P_r\left|h_{u_1r}\right|^2|h_{re}|^2}{P_{u_2}\left|h_{u_2r}\right|^2}\right\} > T\right\} \\ &= g_2\left(A_2+B_2\right), \end{aligned} \tag{49}$$

where g_2, A_2 and B_2 are shown in (50), (51) and (52), in which (51) and (52) are shown at the bottom of the next page.

$$\begin{aligned} g_2 &= \Pr\left\{\frac{\rho_{u_2}\left|h_{u_2e}\right|^2}{\rho_{u_1}\left|h_{u_1e}\right|^2+1} > T, \rho_{u_1}\left|h_{u_1e}\right|^2 < T\right\} \\ &= \frac{\rho_{u_2}\sigma_{u_2e}^2}{\rho_{u_2}\sigma_{u_2e}^2+T\rho_{u_1}\sigma_{u_1e}^2}\left(1-e^{-\frac{\rho_{u_2}\sigma_{u_2e}^2+T\rho_{u_1}\sigma_{u_1e}^2}{\rho_{u_2}\sigma_{u_2e}^2\sigma_{u_1e}^2}\frac{T}{\rho_{u_1}}}\right)e^{-\frac{T}{\rho_{u_2}\sigma_{u_2e}^2}} \end{aligned} \tag{50}$$

3) When both x_1' and x_2' cannot be decoded successfully in the second time slot, the probability of e successfully decoding the signals in the order of $x_1' \to x_2'$ is

$$\begin{aligned} &P_{succ}^{III-1} \\ &= \Pr\left\{\gamma_{e3,4}^{x_1'} > T, \gamma_{e3,4}^{x_2'} > T\right\} \\ &\times \Pr\left\{\frac{\rho_{u_2}\left|h_{u_2e}\right|^2}{\rho_{u_1}\left|h_{u_1e}\right|^2+1} < T, \frac{\rho_{u_1}\left|h_{u_1e}\right|^2}{\rho_{u_2}\left|h_{u_2e}\right|^2+1} < T\right\}, \end{aligned} \tag{53}$$

where the tight upper bounds of $\gamma_{e3,4}^{x_1'}$ and $\gamma_{e3,4}^{x_2'}$ are expressed as

$$\gamma_{e3,4}^{x_1'} \le \min\left\{\begin{array}{l}\frac{P_{u_1}\left|h_{u_1r}\right|^2}{P_{u_2}\left|h_{u_2r}\right|^2}, \rho_{u_1}\left|h_{u_1r}\right|^2, \\ \rho_r|h_{re}|^2, \frac{\rho_r P_{u_1}\left|h_{u_1r}\right|^2|h_{re}|^2}{P_{u_2}\left|h_{u_2r}\right|^2}\end{array}\right\}, \tag{54}$$

$$\gamma_{e3,4}^{x_2'} \le \min\left\{\rho_{u_2}\left|h_{u_2r}\right|^2, \rho_r|h_{re}|^2, \frac{\rho_r P_{u_2}\left|h_{u_2r}\right|^2|h_{re}|^2}{P_{u_1}\left|h_{u_1r}\right|^2}\right\}. \tag{55}$$

$$\begin{aligned} A_1 &= \Pr\left\{P_s|h_{sr}|^2 > P_{th}, \left|h_{u_2r}\right|^2 > \frac{T}{\rho_{u_2}}, |h_{re}|^2 > \frac{\theta T}{2\eta\rho_{th}}, \left|h_{u_1r}\right|^2 < \frac{2\eta\rho_{th}P_{u_2}\left|h_{u_2r}\right|^2|h_{re}|^2}{\theta T P_{u_1}}\right\} \\ &= \Pr\left\{|h_{sr}|^2 > \frac{P_{th}}{P_s}\right\}\int_{\frac{T}{\rho_{u_2}}}^{+\infty}\int_{\frac{\theta T}{2\eta\rho_{th}}}^{+\infty} f_{\left|h_{u_2r}\right|^2}(x) f_{|h_{re}|^2}(y) \Pr\left\{\left|h_{u_1r}\right|^2 < \frac{2\eta\rho_{th}P_{u_2}xy}{\theta T P_{u_1}}\right\}dydx \\ &= e^{-\frac{P_{th}}{P_s\sigma_{sr}^2}}\int_{\frac{T}{\rho_{u_2}}}^{+\infty}\int_{\frac{\theta T}{2\eta\rho_{th}}}^{+\infty}\frac{1}{\sigma_{u_2r}^2}e^{-\frac{x}{\sigma_{u_2r}^2}}\frac{1}{\sigma_{re}^2}e^{-\frac{y}{\sigma_{re}^2}}\left(1-e^{-\frac{2\eta\rho_{th}P_{u_2}xy}{\theta T P_{u_1}\sigma_{u_1r}^2}}\right)dydx \\ &= e^{-\frac{P_{th}}{P_s\sigma_{sr}^2}-\frac{T}{\rho_{u_2}\sigma_{u_2r}^2}-\frac{\theta T}{2\eta\rho_{th}\sigma_{re}^2}} - \frac{\theta T P_{u_1}\sigma_{u_1r}^2}{2\eta\rho_{th}P_{u_2}\sigma_{u_2r}^2\sigma_{re}^2}e^{-\frac{P_{th}}{P_s\sigma_{sr}^2}+\frac{\theta T P_{u_1}\sigma_{u_1r}^2}{2\eta\rho_{th}P_{u_2}\sigma_{u_2r}^2\sigma_{re}^2}} \\ &\quad E_1\left(\frac{\left(P_{u_1}\sigma_{u_1r}^2+P_{u_2}\sigma_{u_2r}^2\right)T\left(\theta P_{u_2}P_{u_1}\sigma_{u_1r}^2+2\eta P_{th}P_{u_2}\sigma_{re}^2\right)}{2\eta P_{th}P_{u_1}\sigma_{u_1r}^2\rho_{u_2}P_{u_2}\sigma_{u_2r}^2\sigma_{re}^2}\right) \end{aligned} \tag{45}$$

$$\begin{aligned} B_1 &= \Pr\left\{P_{\min} < P_s|h_{sr}|^2 \le P_{th}, |h_{re}|^2 > \frac{\theta T}{2\eta P_s|h_{sr}|^2}, \left|h_{u_2r}\right|^2 > \frac{T}{\rho_{u_2}}, \left|h_{u_1r}\right|^2 < \frac{2\eta\rho_s P_{u_2}\left|h_{pr}\right|^2\left|h_{u_2r}\right|^2|h_{re}|^2}{\theta T P_{u_1}}\right\} \\ &= \int_{\frac{P_{\min}}{P_s}}^{\frac{P_{th}}{P_s}}\int_{\frac{T}{\rho_{u_2}}}^{+\infty}\int_{\frac{\theta T}{2\eta\rho_s z}}^{+\infty} f_{|h_{sr}|^2}(z) f_{\left|h_{u_2r}\right|^2}(x) f_{|h_{re}|^2}(y) \Pr\left\{\left|h_{u_1r}\right|^2 < \frac{2\eta\rho_s P_{u_2}zxy}{\theta T P_{u_1}}\right\}dydxdz \\ &= \int_{\frac{P_{\min}}{P_s}}^{\frac{P_{th}}{P_s}}\int_{\frac{T}{\rho_{u_2}}}^{+\infty}\int_{\frac{\theta T}{2\eta\rho_s z}}^{+\infty}\frac{1}{\sigma_{sr}^2}e^{-\frac{z}{\sigma_{sr}^2}}\frac{1}{\sigma_{u_2r}^2}e^{-\frac{x}{\sigma_{u_2r}^2}}\frac{1}{\sigma_{re}^2}e^{-\frac{y}{\sigma_{re}^2}}\left(1-e^{-\frac{2\eta\rho_s P_{u_2}zxy}{\theta T P_{u_1}\sigma_{u_1r}^2}}\right)dydxdz \\ &\approx \frac{1}{\sigma_{sr}^2}Q\left(\frac{P_{\min}}{P_s}, \frac{P_{th}}{P_s}, \frac{1}{\sigma_{sr}^2}, \frac{\theta T}{2\eta\rho_s\sigma_{re}^2}\right)e^{-\frac{T}{\rho_{u_2}\sigma_{u_2r}^2}} - \frac{\theta T P_{u_1}\sigma_{u_1r}^2}{2\eta\rho_s P_{u_2}\sigma_{u_2r}^2\sigma_{sr}^2\sigma_{re}^2}\left[E_1\left(\frac{P_{\min}}{P_s\sigma_{sr}^2}\right)-E_1\left(\frac{P_{th}}{P_s\sigma_{sr}^2}\right)\right] \\ &\quad E_1\left(\frac{\left(P_{u_1}\sigma_{u_1r}^2+P_{u_2}\sigma_{u_2r}^2\right)T}{P_{u_1}\sigma_{u_1r}^2\rho_{u_2}\sigma_{u_2r}^2}\right) \end{aligned} \tag{46}$$

Replace the SNRs in (53) with their corresponding tight upper bounds, and after some manipulation, the upper bound for (53) can be expressed as

$$P_{succ}^{III-1} \le g_3 \Pr\left\{ \begin{array}{l} |h_{re}|^2 > \frac{TP_{u_1}|h_{u_1r}|^2}{\rho_r P_{u_2}|h_{u_2r}|^2}, \\ |h_{u_2r}|^2 > \frac{T}{\rho_{u_2}}, |h_{u_1r}|^2 > \frac{TP_{u_2}|h_{u_2r}|^2}{P_{u_1}} \end{array} \right\} = g_3 (A_3 + B_3), \quad (56)$$

where g_3, A_3 and B_3 are (57), (58) and (59), in which (58) and (59) are shown at the bottom of the next page.

$$g_3 = \Pr\left\{ \frac{\rho_{u_2}|h_{u_2e}|^2}{\rho_{u_1}|h_{u_1e}|^2 + 1} < T, \frac{\rho_{u_1}|h_{u_1e}|^2}{\rho_{u_2}|h_{u_2e}|^2 + 1} < T \right\} = 1 - e^{-\frac{T(\rho_{u_1}+1)}{\rho_{u_2}\sigma_{u_2e}^2}} + \frac{TP_{u_1}\sigma_{u_1e}^2}{TP_{u_1}\sigma_{u_1e}^2 + P_{u_2}\sigma_{u_2e}^2} \times e^{-\frac{T(\rho_{u_1}+1)\sigma_{u_1e}^2 + \rho_{u_2}\sigma_{u_2e}^2}{\sigma_{u_1e}^2\rho_{u_2}\sigma_{u_2e}^2}} - \frac{P_{u_1}\sigma_{u_1e}^2}{P_{u_1}\sigma_{u_1e}^2 + TP_{u_2}\sigma_{u_2e}^2} e^{-\frac{T}{\rho_{u_1}\sigma_{u_1e}^2}}. \quad (57)$$

The probability of e successfully decoding the signals in the order of $x_2' \to x_1'$ in the third time slot is

$$P_{succ}^{III-2} = g_3 \Pr\left\{ \gamma'^{x_2'}_{e3,4} > T, \gamma'^{x_1'}_{e3,4} > T \right\}. \quad (60)$$

Similarly, the tight upper bounds of $\gamma'^{x_2'}_{e3,4}$ and $\gamma'^{x_1'}_{e3,4}$ are

$$\gamma'^{x_2'}_{e3,4} \le \min\left\{ \begin{array}{l} \frac{P_{u_2}|h_{u_2r}|^2}{P_{u_1}|h_{u_1r}|^2}, \rho_{u_2}|h_{u_2r}|^2, \\ \rho_r|h_{re}|^2, \frac{\rho_{u_2}\rho_r|h_{u_2r}|^2|h_{re}|^2}{\rho_{u_1}|h_{u_1r}|^2} \end{array} \right\}, \quad (61)$$

$$\gamma'^{x_1'}_{e3,4} \le \min\left\{ \rho_{u_1}|h_{u_1r}|^2, \rho_r|h_{re}|^2, \frac{\rho_{u_1}\rho_r|h_{u_1r}|^2|h_{re}|^2}{\rho_{u_2}|h_{u_2r}|^2} \right\}. \quad (62)$$

At this time, the upper bound of (60) is

$$P_{succ}^{III-2} \le g_3 (A_4 + B_4), \quad (63)$$

where A_4 and B_4 are shown in (64) and (65), at the bottom of page 12.

In summary, it is known that the upper bound of intercept probability of the considered system is

$$P_{int} \approx P_{succ}^{I} \cdot \left(\begin{array}{l} P_{succ}^{II} + P_{succ}^{I-x_1', II-x_2'} \\ + P_{succ}^{I-x_2', II-x_1'} + P_{succ}^{III-1} + P_{succ}^{III-2} \end{array} \right). \quad (66)$$

IV. PERFORMANCE ANALYSIS IN HIGH SNR

A. OUTAGE PROBABILITY

Base on the fact that the $e^{-x} \approx 1 - x$ in the case of $x \to 0$, using the reciprocal of SNR as an exponential function for Taylor expansion, ignoring the higher-order term of the

$$\begin{aligned} A_2 &= \Pr\left\{ P_s|h_{sr}|^2 > P_{th}, |h_{u_1r}|^2 > \frac{T}{\rho_{u_1}}, |h_{re}|^2 > \frac{T}{\rho_r}, |h_{u_2r}|^2 < \frac{\rho_{u_1}P_r}{TP_{u_2}}|h_{u_1r}|^2|h_{re}|^2 \right\} \\ &= e^{-\frac{P_{th}}{P_s\sigma_{sr}^2}} \int_{\frac{T}{\rho_{u_1}}}^{+\infty} \int_{\frac{\theta T}{2\eta\rho_{th}}}^{+\infty} \frac{1}{\sigma_{u_1r}^2} e^{-\frac{x}{\sigma_{u_1r}^2}} \frac{1}{\sigma_{re}^2} e^{-\frac{y}{\sigma_{re}^2}} \left(1 - e^{-\frac{\rho_{u_1}2\eta P_{th}xy}{\theta TP_{u_2}\sigma_{u_2r}^2}} \right) dydx \\ &= e^{-\frac{P_{th}}{P_s\sigma_{sr}^2} - \frac{T}{\rho_{u_1}\sigma_{u_1r}^2} - \frac{\theta T}{2\eta\rho_{th}\sigma_{re}^2}} \\ &\quad - \frac{\theta TP_{u_2}\sigma_{u_2r}^2}{2\eta\rho_{th}P_{u_1}\sigma_{u_1r}^2\sigma_{re}^2} e^{-\frac{P_{th}}{P_s\sigma_{sr}^2} + \frac{\theta TP_{u_2}\sigma_{u_2r}^2}{2\eta\rho_{th}P_{u_1}\sigma_{u_1r}^2\sigma_{re}^2}} E_1\left(\frac{\left(P_{u_2}\sigma_{u_2r}^2 + P_{u_1}\sigma_{u_1r}^2\right) T\left(\theta P_{u_1}P_{u_2}\sigma_{u_2r}^2 + 2\eta P_{th}P_{u_1}\sigma_{re}^2\right)}{2\eta P_{th}\rho_{u_1}P_{u_1}\sigma_{u_1r}^2P_{u_2}\sigma_{u_2r}^2\sigma_{re}^2} \right) \end{aligned} \quad (51)$$

$$\begin{aligned} B_2 &= \Pr\left\{ P_{\min} < P_s|h_{sr}|^2 \le P_{th}, |h_{u_1r}|^2 > \frac{T}{\rho_{u_1}}, |h_{re}|^2 > \frac{T}{\rho_r}, |h_{u_2r}|^2 < \frac{\rho_{u_1}P_r}{TP_{u_2}}|h_{u_1r}|^2|h_{re}|^2 \right\} \\ &= \int_{\frac{P_{\min}}{P_s}}^{\frac{P_{th}}{P_s}} \int_{\frac{T}{\rho_{u_1}}}^{+\infty} \int_{\frac{\theta T}{2\eta\rho_s z}}^{+\infty} f_{|h_{sr}|^2}(z) f_{|h_{u_1r}|^2}(x) f_{|h_{re}|^2}(y) \Pr\left\{ |h_{u_2r}|^2 < \frac{2\eta\rho_s P_{u_1} zxy}{\theta TP_{u_2}} \right\} dydxdz \\ &\approx \int_{\frac{P_{\min}}{P_s}}^{\frac{P_{th}}{P_s}} \frac{1}{\sigma_{sr}^2} e^{-\frac{z}{\sigma_{sr}^2} - \frac{\theta T}{2\eta\rho_s\sigma_{re}^2 z}} dz \int_{\frac{T}{\rho_{u_1}}}^{+\infty} \frac{1}{\sigma_{u_1r}^2} e^{-\frac{x}{\sigma_{u_1r}^2}} dx - \frac{\theta TP_{u_2}\sigma_{u_2r}^2}{2\eta\rho_{u_1}P_s\sigma_{re}^2} \int_{\frac{P_{\min}}{P_s}}^{\frac{P_{th}}{P_s}} \frac{1}{\sigma_{sr}^2 z} e^{-\frac{z}{\sigma_{sr}^2}} dz \int_{\frac{T}{\rho_{u_1}}}^{+\infty} \frac{1}{\sigma_{u_1r}^2 x} e^{-\frac{P_{u_1}\sigma_{u_1r}^2 + P_{u_2}\sigma_{u_2r}^2}{P_{u_2}\sigma_{u_2r}^2\sigma_{u_1r}^2}x} dx \\ &= \frac{1}{\sigma_{sr}^2} Q\left(\frac{P_{\min}}{P_s}, \frac{P_{th}}{P_s}, \frac{1}{\sigma_{sr}^2}, \frac{\theta T}{2\eta\rho_s\sigma_{re}^2} \right) e^{-\frac{T}{\rho_{u_1}\sigma_{u_1r}^2}} - \frac{\theta TP_{u_2}\sigma_{u_2r}^2}{2\eta P_s\rho_{u_1}\sigma_{u_1r}^2\sigma_{sr}^2\sigma_{re}^2} \left[E_1\left(\frac{P_{\min}}{P_s\sigma_{sr}^2} \right) - E_1\left(\frac{P_{th}}{P_s\sigma_{sr}^2} \right) \right] \\ &\quad E_1\left(\frac{\left(P_{u_1}\sigma_{u_1r}^2 + P_{u_2}\sigma_{u_2r}^2\right) T}{P_{u_2}\sigma_{u_2r}^2\rho_{u_1}\sigma_{u_1r}^2} \right) \end{aligned} \quad (52)$$

reciprocal of SNR and retaining its lower-order term, we can obtain

$$I_1 \approx e^{-\frac{P_{th}}{P_s\sigma_{sr}^2}}. \tag{67}$$

In addition, when $b \to 0$,

$$Q(x_0, x_1, a, b) \approx \int_{x_0}^{x_1} e^{-ax}\left(1-\frac{b}{x}\right)dx \approx \frac{e^{-ax_0}-e^{-ax_1}}{a}. \tag{68}$$

Therefore, when $P_{u_1} > P_{u_2}$, after some manipulation,

$$I_2 \approx e^{-\frac{P_{\min}}{P_s\sigma_{sr}^2}} - e^{-\frac{P_{th}}{P_s\sigma_{sr}^2}}. \tag{69}$$

From (27), it can be seen that in the high SNR region, $P_{out} \approx 1-(I_1+I_2)$, and then (67) and (69) are substituted into it, we can be obtained $P_{out} \approx 1-\exp\left[-P_{\min}/\left(P_s\sigma_{sr}^2\right)\right]$. Similarly, when $P_{u_1} < P_{u_2}$, at high SNR, $P_{out} \approx 1-\exp\left[-P_{\min}/\left(P_s\sigma_{sr}^2\right)\right]$. In summary, the approximate outage probability of the considered system in the high SNR regime can be simplified as

$$P_{out} \approx 1 - e^{-\frac{P_{\min}}{P_s\sigma_{sr}^2}}. \tag{70}$$

From (70), we can see that the outage probability of the considered system is only determined by P_s, $P_{\min}$ and σ_{sr}^2 in high SNR.

B. INTERCEPT PROBABILITY

In the high SNR region, $P_{succ}^{I} \approx 1$. In the second time slot, the probability of successful decoding can be approximated as

$$P_{succ}^{II} \approx \frac{P_{u_1}\sigma_{u_1e}^2}{P_{u_1}\sigma_{u_1e}^2 + TP_{u_2}\sigma_{u_2e}^2} + \frac{P_{u_2}\sigma_{u_2e}^2}{P_{u_2}\sigma_{u_2e}^2 + TP_{u_1}\sigma_{u_1e}^2}. \tag{71}$$

In the third time slot:

1) (44)-(46) in the high SNR regime can be approximated by

$$g_1 \approx \frac{T}{\rho_{u_2}\sigma_{u_2e}^2}, \tag{72}$$

$$\begin{aligned}
A_3 &= \Pr\left\{P_s|h_{sr}|^2 > P_{th}, |h_{re}|^2 > \frac{\theta TP_{u_1}\left|h_{u_1r}\right|^2}{2\eta\rho_{th}P_{u_2}\left|h_{u_2r}\right|^2}, \left|h_{u_2r}\right|^2 > \frac{T}{\rho_{u_2}}, \left|h_{u_1r}\right|^2 > \frac{TP_{u_2}\left|h_{u_2r}\right|^2}{P_{u_1}}\right\} \\
&= e^{-\frac{P_{th}}{P_s\sigma_{sr}^2}}\int_{\frac{T}{\rho_{u_2}}}^{+\infty}\frac{1}{\sigma_{u_2r}^2}\frac{2\eta\rho_{th}P_{u_2}\sigma_{re}^2 y}{2\eta\rho_{th}P_{u_2}\sigma_{re}^2 y+\theta TP_{u_1}\sigma_{u_1r}^2}e^{-\frac{y}{\sigma_{u_2r}^2}-\frac{2\eta\rho_{th}P_{u_2}\sigma_{re}^2 y+\theta TP_{u_1}\sigma_{u_1r}^2}{2\eta\rho_{th}P_{u_1}\sigma_{u_1r}^2\sigma_{re}^2}T}dy \\
&= e^{-\frac{P_{th}}{P_s\sigma_{sr}^2}+\frac{\theta TP_{u_1}\sigma_{u_1r}^2}{2\eta\rho_{th}P_{u_2}\sigma_{u_2r}^2\sigma_{re}^2}}\left(\begin{array}{l}\frac{P_{u_1}\sigma_{u_1r}^2}{P_{u_1}\sigma_{u_1r}^2+TP_{u_2}\sigma_{u_2r}^2}e^{-\frac{\left(P_{u_1}\sigma_{u_1r}^2+TP_{u_2}\sigma_{u_2r}^2\right)T\left(2\eta P_{th}\sigma_{re}^2+\theta P_{u_1}\sigma_{u_1r}^2\right)}{2\eta\rho_{th}P_{u_1}\sigma_{u_1r}^2P_{u_2}\sigma_{u_2r}^2\sigma_{re}^2}}- \\ \frac{\theta TP_{u_1}\sigma_{u_1r}^2}{2\eta\rho_{th}P_{u_2}\sigma_{u_2r}^2\sigma_{re}^2}E_1\left(\frac{\left(P_{u_1}\sigma_{u_1r}^2+TP_{u_2}\sigma_{u_2r}^2\right)T\left(2\eta P_{th}\sigma_{re}^2+\theta P_{u_1}\sigma_{u_1r}^2\right)}{2\eta\rho_{th}P_{u_1}\sigma_{u_1r}^2P_{u_2}\sigma_{u_2r}^2\sigma_{re}^2}\right)\end{array}\right)
\end{aligned} \tag{58}$$

$$\begin{aligned}
B_3 &= \Pr\left\{\frac{P_{\min}}{P_s} < |h_{sr}|^2 \le \frac{P_{th}}{P_s}, |h_{re}|^2 > \frac{\theta TP_{u_1}\left|h_{u_1r}\right|^2}{2\eta\rho_sP_{u_2}|h_{sr}|^2\left|h_{u_2r}\right|^2}, \left|h_{u_2r}\right|^2 > \frac{T}{\rho_{u_2}}, \left|h_{u_1r}\right|^2 > \frac{TP_{u_2}\left|h_{u_2r}\right|^2}{P_{u_1}}\right\} \\
&= \int_{\frac{P_{\min}}{P_s}}^{\frac{P_{th}}{P_s}}\int_{\frac{T}{\rho_{u_2}}}^{+\infty}\frac{1}{\sigma_{sr}^2}e^{-\frac{z}{\sigma_{sr}^2}}\frac{1}{\sigma_{u_2r}^2}\frac{2\eta\rho_sP_{u_2}\sigma_{re}^2 zy}{2\eta\rho_sP_{u_2}\sigma_{re}^2 zy+\theta TP_{u_1}\sigma_{u_1r}^2}e^{-\frac{y}{\sigma_{u_2r}^2}-\frac{2\eta\rho_sP_{u_2}\sigma_{re}^2 zy+\theta TP_{u_1}\sigma_{u_1r}^2}{2\eta\rho_sP_{u_1}\sigma_{u_1r}^2\sigma_{re}^2 z}T}dydz \\
&\approx \frac{1}{\sigma_{sr}^2\sigma_{u_2r}^2}\int_{\frac{P_{\min}}{P_s}}^{\frac{P_{th}}{P_s}}e^{-\frac{z}{\sigma_{sr}^2}-\frac{\theta T^2}{2\eta\rho_s\sigma_{re}^2 z}}dz\int_{\frac{T}{\rho_{u_2}}}^{+\infty}e^{-\frac{P_{u_1}\sigma_{u_1r}^2+TP_{u_2}\sigma_{u_2r}^2}{P_{u_1}\sigma_{u_1r}^2\sigma_{u_2r}^2}y}dy \\
&\quad - \frac{1}{\sigma_{sr}^2\sigma_{u_2r}^2}\frac{\theta TP_{u_1}\sigma_{u_1r}^2}{2\eta\rho_sP_{u_2}\sigma_{re}^2}\int_{\frac{P_{\min}}{P_s}}^{\frac{P_{th}}{P_s}}\frac{1}{z}e^{-\frac{z}{\sigma_{sr}^2}-\frac{\theta T^2}{2\eta\rho_s\sigma_{re}^2 z}}dz\int_{\frac{T}{\rho_{u_2}}}^{+\infty}\frac{1}{y}e^{-\frac{P_{u_1}\sigma_{u_1r}^2+TP_{u_2}\sigma_{u_2r}^2}{P_{u_1}\sigma_{u_1r}^2\sigma_{u_2r}^2}y}dy \\
&= \frac{1}{\sigma_{sr}^2}\frac{P_{u_1}\sigma_{u_1r}^2}{P_{u_1}\sigma_{u_1r}^2+TP_{u_2}\sigma_{u_2r}^2}Q\left(\frac{P_{\min}}{P_s}, \frac{P_{th}}{P_s}, \frac{1}{\sigma_{sr}^2}, \frac{\theta T^2}{2\eta\rho_s\sigma_{re}^2}\right)e^{-\frac{P_{u_1}\sigma_{u_1r}^2+TP_{u_2}\sigma_{u_2r}^2}{P_{u_1}\sigma_{u_1r}^2\sigma_{u_2r}^2}\frac{T}{\rho_{u_2}}} - \frac{\theta TP_{u_1}\sigma_{u_1r}^2}{2\eta\rho_sP_{u_2}\sigma_{sr}^2\sigma_{u_2r}^2\sigma_{re}^2} \\
&\quad E_1\left(\frac{P_{u_1}\sigma_{u_1r}^2+TP_{u_2}\sigma_{u_2r}^2}{P_{u_1}\sigma_{u_1r}^2\sigma_{u_2r}^2}\frac{T}{\rho_{u_2}}\right) \\
&\quad \times\left[\left(1+\frac{\theta T^2}{2\eta\rho_s\sigma_{sr}^2\sigma_{re}^2}\right)\left(E_1\left(\frac{P_{\min}}{P_s\sigma_{sr}^2}\right)-E_1\left(\frac{P_{th}}{P_s\sigma_{sr}^2}\right)\right)+\frac{\theta T^2}{2\eta\rho_s\sigma_{re}^2}\left(\frac{P_s}{P_{th}}e^{-\frac{P_{th}}{P_s\sigma_{sr}^2}}-\frac{P_s}{P_{\min}}e^{-\frac{P_{\min}}{P_s\sigma_{sr}^2}}\right)\right]
\end{aligned} \tag{59}$$

$$A_1 \approx e^{-\frac{P_{th}}{P_s\sigma_{sr}^2}}, \tag{73}$$

$$B_1 \approx e^{-\frac{P_{\min}}{P_s\sigma_{sr}^2}} - e^{-\frac{P_{th}}{P_s\sigma_{sr}^2}}. \tag{74}$$

Then substitute (68)-(70) into (42) to obtain

$$P_{succ}^{I-x_1',II-x_2'} \approx \frac{T}{\rho_{u_2}\sigma_{u_2e}^2} e^{-\frac{P_{\min}}{P_s\sigma_{sr}^2}}. \tag{75}$$

2) (50)-(52) in the high SNR regime can be approximated by

$$g_2 \approx \frac{T}{\rho_{u_1}\sigma_{u_1e}^2}, \tag{76}$$

$$A_2 \approx e^{-\frac{P_{th}}{P_s\sigma_{sr}^2}}, \tag{77}$$

$$B_2 \approx e^{-\frac{P_{\min}}{P_s\sigma_{sr}^2}} - e^{-\frac{P_{th}}{P_s\sigma_{sr}^2}}. \tag{78}$$

Therefore, the probability of e successfully decoding x_1' and x_2' in that case can be approximated as

$$P_{succ}^{I-x_2',II-x_1'} \approx \frac{T}{\rho_{u_1}\sigma_{u_1e}^2} e^{-\frac{P_{\min}}{P_s\sigma_{sr}^2}}. \tag{79}$$

3) (57)-(59) in the high SNR regime can be approximated by

$$g_3 \approx \frac{TP_{u_2}\sigma_{u_2e}^2}{P_{u_1}\sigma_{u_1e}^2 + TP_{u_2}\sigma_{u_2e}^2} - e^{-\frac{TP_{u_1}}{P_{u_2}\sigma_{u_2e}^2}} + \frac{TP_{u_1}\sigma_{u_1e}^2}{TP_{u_1}\sigma_{u_1e}^2 + P_{u_2}\sigma_{u_2e}^2} e^{-\frac{TP_{u_1}\sigma_{u_1e}^2 + P_{u_2}\sigma_{u_2e}^2}{\sigma_{u_1e}^2 P_{u_2}\sigma_{u_2e}^2}}, \tag{80}$$

$$\begin{aligned}
A_4 &= \Pr\left\{P_s|h_{sr}|^2 > P_{th}, |h_{re}|^2 > \frac{\theta TP_{u_2}|h_{u_2r}|^2}{2\eta\rho_{th}P_{u_1}|h_{u_1r}|^2}, |h_{u_1r}|^2 > \frac{T}{\rho_{u_1}}, |h_{u_2r}|^2 > \frac{TP_{u_1}}{P_{u_2}}|h_{u_1r}|^2\right\} \\
&= \Pr\left\{|h_{sr}|^2 > \frac{P_{th}}{P_s}\right\} \int_{\frac{T}{\rho_{u_1}}}^{+\infty} \int_{\frac{TP_{u_1}y}{P_{u_2}}}^{+\infty} f_{|h_{u_1r}|^2}(y) f_{|h_{u_2r}|^2}(x) \Pr\left\{|h_{re}|^2 > \frac{\theta TP_{u_2}x}{2\eta\rho_{th}P_{u_1}y}\right\} dxdy \\
&= e^{-\frac{P_{th}}{P_s\sigma_{sr}^2}} \int_{\frac{T}{\rho_{u_1}}}^{+\infty} \frac{1}{\sigma_{u_1r}^2} \frac{2\eta P_{th}\rho_{u_1}\sigma_{re}^2 y}{2\eta P_{th}\rho_{u_1}\sigma_{re}^2 y + \theta TP_{u_2}\sigma_{u_2r}^2} e^{-\frac{y}{\sigma_{u_1r}^2} - \frac{2\eta P_{th}\rho_{u_1}\sigma_{re}^2 y + \theta TP_{u_2}\sigma_{u_2r}^2}{2\eta P_{th}\rho_{u_2}\sigma_{u_2r}^2\sigma_{re}^2}T} dy \\
&= e^{-\frac{P_{th}}{P_s\sigma_{sr}^2} - \frac{\theta T^2}{2\eta\rho_{th}\sigma_{re}^2}} \int_{\frac{T}{\rho_{u_1}}}^{+\infty} \frac{1}{\sigma_{u_1r}^2} \left(1 - \frac{\theta TP_{u_2}\sigma_{u_2r}^2}{2\eta P_{th}\rho_{u_1}\sigma_{re}^2 y + \theta TP_{u_2}\sigma_{u_2r}^2}\right) e^{-\frac{P_{u_2}\sigma_{u_2r}^2 + TP_{u_1}\sigma_{u_1r}^2}{\sigma_{u_1r}^2 P_{u_2}\sigma_{u_2r}^2} y} dy \\
&= e^{-\frac{P_{th}}{P_s\sigma_{sr}^2} + \frac{\theta TP_{u_2}\sigma_{u_2r}^2}{2\eta\rho_{th}P_{u_1}\sigma_{u_1r}^2\sigma_{re}^2}} \left(\frac{P_{u_2}\sigma_{u_2r}^2}{P_{u_2}\sigma_{u_2r}^2 + TP_{u_1}\sigma_{u_1r}^2} e^{-\frac{\left(P_{u_2}\sigma_{u_2r}^2 + TP_{u_1}\sigma_{u_1r}^2\right)T\left(2\eta P_{th}\sigma_{re}^2 + \theta P_{u_2}\sigma_{u_2r}^2\right)}{2\eta P_{th}\rho_{u_1}\sigma_{u_1r}^2 P_{u_2}\sigma_{u_2r}^2\sigma_{re}^2}} - \right. \\
&\quad \left. \frac{\theta TP_{u_2}\sigma_{u_2r}^2}{2\eta\rho_{th}P_{u_1}\sigma_{u_1r}^2\sigma_{re}^2} E_1\left(\frac{\left(P_{u_2}\sigma_{u_2r}^2 + TP_{u_1}\sigma_{u_1r}^2\right)T\left(2\eta P_{th}\sigma_{re}^2 + \theta P_{u_2}\sigma_{u_2r}^2\right)}{2\eta P_{th}\rho_{u_1}\sigma_{u_1r}^2 P_{u_2}\sigma_{u_2r}^2\sigma_{re}^2}\right)\right)
\end{aligned} \tag{64}$$

$$\begin{aligned}
B_4 &= \Pr\left\{\frac{P_{\min}}{P_s} < |h_{sr}|^2 \le \frac{P_{th}}{P_s}, |h_{re}|^2 > \frac{\theta TP_{u_2}|h_{u_2r}|^2}{2\eta\rho_s|h_{sr}|^2 P_{u_1}|h_{u_1r}|^2}, |h_{u_1r}|^2 > \frac{T}{\rho_{u_1}}, |h_{u_2r}|^2 > \frac{TP_{u_1}}{P_{u_2}}|h_{u_1r}|^2\right\} \\
&= \int_{\frac{P_{\min}}{P_s}}^{\frac{P_{th}}{P_s}} \int_{\frac{T}{\rho_{u_1}}}^{+\infty} \int_{\frac{TP_{u_1}y}{P_{u_2}}}^{+\infty} f_{|h_{sr}|^2}(z) f_{|h_{u_1r}|^2}(y) f_{|h_{u_2r}|^2}(x) \Pr\left\{|h_{re}|^2 > \frac{\theta TP_{u_2}x}{2\eta\rho_s z P_{u_1}y}\right\} dxdydz \\
&\approx \frac{1}{\sigma_{sr}^2\sigma_{u_1r}^2} \int_{\frac{P_{\min}}{P_s}}^{\frac{P_{th}}{P_s}} e^{-\frac{z}{\sigma_{sr}^2} - \frac{\theta T^2}{2\eta\rho_s\sigma_{re}^2 z}} dz \int_{\frac{T}{\rho_{u_1}}}^{+\infty} e^{-\frac{P_{u_2}\sigma_{u_2r}^2 + TP_{u_1}\sigma_{u_1r}^2}{P_{u_2}\sigma_{u_2r}^2\sigma_{u_1r}^2} y} dy \\
&\quad - \frac{1}{\sigma_{sr}^2} \frac{\theta TP_{u_2}\sigma_{u_2r}^2}{2\eta\rho_s P_{u_1}\sigma_{u_1r}^2\sigma_{re}^2} \int_{\frac{P_{\min}}{P_s}}^{\frac{P_{th}}{P_s}} \frac{1}{z} e^{-\frac{z}{\sigma_{sr}^2} - \frac{\theta T^2}{2\eta\rho_s\sigma_{re}^2 z}} dz \int_{\frac{T}{\rho_{u_1}}}^{+\infty} \frac{1}{y} e^{-\frac{P_{u_2}\sigma_{u_2r}^2 + TP_{u_1}\sigma_{u_1r}^2}{P_{u_2}\sigma_{u_2r}^2\sigma_{u_1r}^2} y} dy \\
&\approx \frac{1}{\sigma_{sr}^2} \frac{P_{u_2}\sigma_{u_2r}^2}{P_{u_2}\sigma_{u_2r}^2 + TP_{u_1}\sigma_{u_1r}^2} Q\left(\frac{P_{\min}}{P_s}, \frac{P_{th}}{P_s}, \frac{1}{\sigma_{sr}^2}, \frac{\theta T^2}{2\eta\rho_s\sigma_{re}^2}\right) e^{-\frac{P_{u_2}\sigma_{u_2r}^2 + TP_{u_1}\sigma_{u_1r}^2}{P_{u_2}\sigma_{u_2r}^2\sigma_{u_1r}^2}\frac{T}{\rho_{u_1}}} - \frac{\theta TP_{u_2}\sigma_{u_2r}^2}{2\eta\rho_s\sigma_{sr}^2 P_{u_1}\sigma_{u_1r}^2\sigma_{re}^2} \\
&\quad E_1\left(\frac{P_{u_2}\sigma_{u_2r}^2 + TP_{u_1}\sigma_{u_1r}^2}{P_{u_2}\sigma_{u_2r}^2\sigma_{u_1r}^2}\frac{T}{\rho_{u_1}}\right) \\
&\quad \times \left[\left(1 + \frac{\theta T^2}{2\eta\rho_s\sigma_{sr}^2\sigma_{re}^2}\right)\left(E_1\left(\frac{P_{\min}}{P_s\sigma_{sr}^2}\right) - E_1\left(\frac{P_{th}}{P_s\sigma_{sr}^2}\right)\right) + \frac{\theta T^2}{2\eta\rho_s\sigma_{re}^2}\left(\frac{P_s}{P_{th}}e^{-\frac{P_{th}}{P_s\sigma_{sr}^2}} - \frac{P_s}{P_{\min}}e^{-\frac{P_{\min}}{P_s\sigma_{sr}^2}}\right)\right]
\end{aligned} \tag{65}$$

$$A_3 \approx \frac{P_{u_1}\sigma_{u_1r}^2}{P_{u_1}\sigma_{u_1r}^2 + TP_{u_2}\sigma_{u_2r}^2} e^{-\frac{P_{th}}{P_s\sigma_{sr}^2}}, \tag{81}$$

$$B_3 \approx \frac{P_{u_1}\sigma_{u_1r}^2}{P_{u_1}\sigma_{u_1r}^2 + TP_{u_2}\sigma_{u_2r}^2} \left(e^{-\frac{P_{\min}}{P_s\sigma_{sr}^2}} - e^{-\frac{P_{th}}{P_s\sigma_{sr}^2}} \right). \tag{82}$$

Thus, (56) can be approximated as

$$P_{succ}^{III-1} \approx \left(\begin{array}{l} \frac{TP_{u_2}\sigma_{u_2e}^2}{P_{u_1}\sigma_{u_1e}^2+TP_{u_2}\sigma_{u_2e}^2} - e^{-\frac{TP_{u_1}}{P_{u_2}\sigma_{u_2e}^2}} + \\ \frac{TP_{u_1}\sigma_{u_1e}^2}{TP_{u_1}\sigma_{u_1e}^2+P_{u_2}\sigma_{u_2e}^2} e^{-\frac{TP_{u_1}\sigma_{u_1e}^2+P_{u_2}\sigma_{u_2e}^2}{\sigma_{u_1e}^2P_{u_2}\sigma_{u_2e}^2}} \end{array} \right) \times \frac{P_{u_1}\sigma_{u_1r}^2}{P_{u_1}\sigma_{u_1r}^2 + TP_{u_2}\sigma_{u_2r}^2} e^{-\frac{P_{\min}}{P_s\sigma_{sr}^2}}. \tag{83}$$

(64) and (65) can be approximated by

$$A_4 \approx \frac{P_{u_2}\sigma_{u_2r}^2}{P_{u_2}\sigma_{u_2r}^2 + TP_{u_1}\sigma_{u_1r}^2} e^{-\frac{P_{th}}{P_s\sigma_{sr}^2}}, \tag{84}$$

$$B_4 \approx \frac{P_{u_2}\sigma_{u_2r}^2}{P_{u_2}\sigma_{u_2r}^2 + TP_{u_1}\sigma_{u_1r}^2} \left(e^{-\frac{P_{\min}}{P_s\sigma_{sr}^2}} - e^{-\frac{P_{th}}{P_s\sigma_{sr}^2}} \right). \tag{85}$$

Substituting (80), (84) and (85) into (63), we obtain

$$P_{succ}^{III-2} \approx \left(\begin{array}{l} \frac{TP_{u_2}\sigma_{u_2e}^2}{P_{u_1}\sigma_{u_1e}^2+TP_{u_2}\sigma_{u_2e}^2} - e^{-\frac{TP_{u_1}}{P_{u_2}\sigma_{u_2e}^2}} + \\ \frac{TP_{u_1}\sigma_{u_1e}^2}{TP_{u_1}\sigma_{u_1e}^2+P_{u_2}\sigma_{u_2e}^2} e^{-\frac{TP_{u_1}\sigma_{u_1e}^2+P_{u_2}\sigma_{u_2e}^2}{\sigma_{u_1e}^2P_{u_2}\sigma_{u_2e}^2}} \end{array} \right) \times \frac{P_{u_2}\sigma_{u_2r}^2}{P_{u_2}\sigma_{u_2r}^2 + TP_{u_1}\sigma_{u_1r}^2} e^{-\frac{P_{\min}}{P_s\sigma_{sr}^2}}. \tag{86}$$

In summary, by substituting $P_{succ}^{I} \approx 1$, (71), (75), (79), (83) and (86) into (66), and after some manipulation, the approximate intercept probability of the considered system in the high SNR regime can be expressed as

$$\begin{aligned} P_{int} &\approx \frac{P_{u_1}\sigma_{u_1e}^2}{P_{u_1}\sigma_{u_1e}^2 + TP_{u_2}\sigma_{u_2e}^2} + \frac{P_{u_2}\sigma_{u_2e}^2}{P_{u_2}\sigma_{u_2e}^2 + TP_{u_1}\sigma_{u_1e}^2} \\ &+ \left(\begin{array}{l} \frac{TP_{u_2}\sigma_{u_2e}^2}{P_{u_1}\sigma_{u_1e}^2+TP_{u_2}\sigma_{u_2e}^2} - e^{-\frac{TP_{u_1}}{P_{u_2}\sigma_{u_2e}^2}} \\ + \frac{TP_{u_1}\sigma_{u_1e}^2}{TP_{u_1}\sigma_{u_1e}^2+P_{u_2}\sigma_{u_2e}^2} e^{-\frac{TP_{u_1}\sigma_{u_1e}^2+P_{u_2}\sigma_{u_2e}^2}{\sigma_{u_1e}^2P_{u_2}\sigma_{u_2e}^2}} \end{array} \right) \\ &\times \left(\frac{P_{u_1}\sigma_{u_1r}^2}{P_{u_1}\sigma_{u_1r}^2+TP_{u_2}\sigma_{u_2r}^2} + \frac{P_{u_2}\sigma_{u_2r}^2}{P_{u_2}\sigma_{u_2r}^2+TP_{u_1}\sigma_{u_1r}^2} \right) e^{-\frac{P_{\min}}{P_s\sigma_{sr}^2}}. \end{aligned} \tag{87}$$

V. SIMULATION ANALYSIS

In this section, numerical simulations are provided to show the performance of the proposed protocol in this system and simulation results are discussed. During the simulation, we assume $\sigma_{ru_1}^2 = \sigma_{ru_2}^2 = \sigma_{re}^2 = \sigma_{u_1e}^2 = \sigma_{u_2e}^2 = 1$, $\sigma_{su_1}^2 = \sigma_{su_2}^2 = 5$, $\sigma_{sr}^2 = 10$, $P_{u_1} = 40$, $P_{u_2} = 20$ and $\eta = 0.7$. We evaluate the performance of the proposed model and corresponding protocol in terms of the outage probability and the intercept probability as the function of the $SNR = 10\log_2\left(1/N_0\right)$ for the targeted SNR transmission threshold $T = 15$. Monte Carlo simulation is used to verify the effectiveness of theoretical derivation. Moreover, For comparison, a NXOR protocol is provided as a benchmark to show the superiority of the proposed protocol, in which the two users directly send their own data without undergoing bit-level XOR processing with the data sent by s.

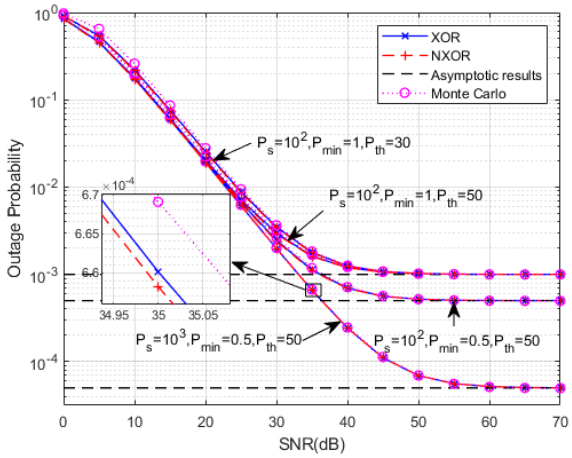

FIGURE 3. Outage probability versus SNR with different P_s, P_{min} and P_{th}, where $\alpha = 0.4$.

Fig.3 depicts the outage probability of the considered system versus SNR with different P_s, P_{min} and P_{th} in the case of $\alpha = 0.4$. It can be found from the figure that the Monte Carlo curves basically match with the tight lower bound of results, which verifies the correctness of the previous derived results. In addition, it can be observed that the outage probability of XOR is basically the same as that of NXOR. Moreover, the outage probability decreases with the increasing of SNR and finally reach the performance bound, which matches the asymptotic results well in the high SNR regime. From the figure, we also can see that the performance bound in the case of $P_s = 10^3$ is lower than that in the case of $P_s = 10^2$, the performance bound in the case of $P_{min} = 0.5$ is lower than that in the case of $P_{min} = 1$, and the outage performance in the case of $P_{th} = 50$ is better than that in the case of $P_{th} = 30$ in low SNR, but the value P_{th} has no effect on the performance bound, which coincides with the asymptotic results in (70).

Fig.4 shows the intercept probability versus SNR with different σ_{se}^2 in the case of $P_s = 10^3$, $P_{min} = 0.5$, $P_{th} = 50$ and $\alpha = 0.4$. From the figure, we can see that the upper bounds of the intercept probability is very close to the Monte Carlo simulation curves, which verifies the effectiveness of theoretical derivation of the upper bound of the intercept probability. Moreover, it can be found that the intercept probability become smaller and smaller when σ_{se}^2 decreases, and the security of the system with XOR is much higher than that of the system without XOR in the case of σ_{se}^2 being smaller.

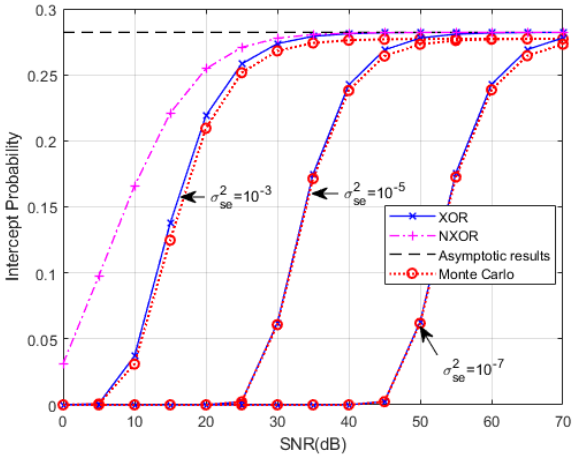

FIGURE 4. Intercept probability versus SNR with different σ_{se}^2, where $P_s = 10^3$, $P_{min} = 0.5$, $P_{th} = 50$ and $\alpha = 0.4$.

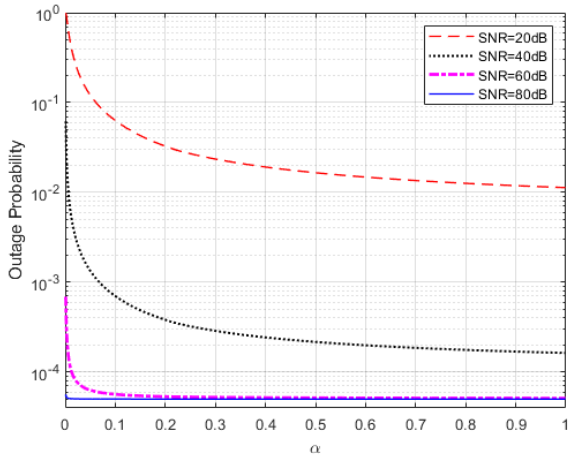

FIGURE 5. Outage probability versus α with different SNR, where $P_s = 10^3$, $P_{min} = 0.5$ and $P_{th} = 50$.

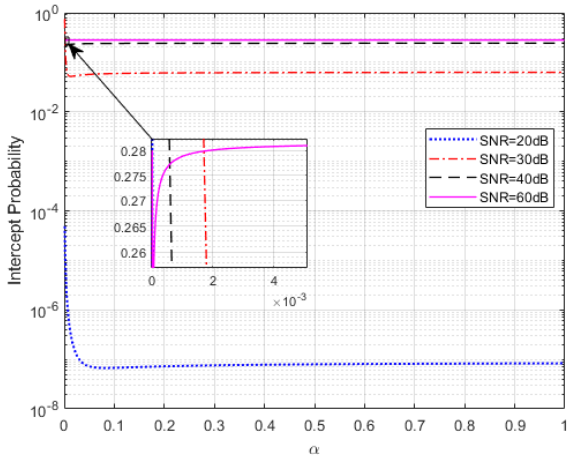

FIGURE 6. Intercept probability versus α with different SNR, where $P_s = 10^3$, $P_{min} = 0.5$, $P_{th} = 50$ and $\sigma_{se}^2 = 10^{-5}$.

Fig.5 and Fig.6 respectively show the influence of α on the outage performance and the intercept performance with different SNR. It can be found from Fig.5 that the outage probability becomes smaller as α increases, but in the high SNR regime, the outage probability is little affected by the change of α value and nearly tends to a fixed value. From Fig.6, we can see that as the value of α increases, the intercept probability sharply decreases and then slowly increases, but the growth of intercept probability are very insignificant. Specially in high SNR, the intercept probability nearly tends to a constant.

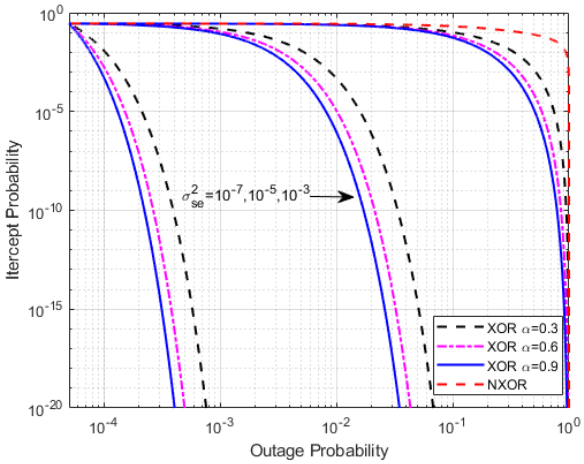

FIGURE 7. The security-reliability tradeoff with different σ_{se}^2 and α, where $P_s = 10^3$, $P_{min} = 0.5$ and $P_{th} = 50$.

It can be seen from Fig.3 and Fig.4 that the outage probability and intercept probability are decreasing and increasing functions of SNR, respectively. This implies that there exists a tradeoff between the intercept probability and outage probability of the considered system. Based on this observation, we give the security-reliability tradeoff with different σ_{se}^2 and α in the case of $P_s = 10^3$, $P_{min} = 0.5$ and $P_{th} = 50$ in Fig.7. It can be seen that with the smaller σ_{se}^2, the XOR scheme much outperforms the NXOR scheme in terms of the security-reliability tradeoff, indicating the advantage of the proposed protocol. We also can see that the security-reliability tradeoff performance of the considered system with the proposed protocol is obviously improved as σ_{se}^2 decreases and α increases.

VI. CONCLUSION

In order to improve the security and reliability of the energy-constrained two-way AF relay system, an independent energy source that is also a signal source providing secret key is introduced into the model in this paper. Based on the non-linear characteristics of the actual circuit, we analyze the tight lower bound of the outage probability and the upper bound of the intercept probability of the system under the Rayleigh channel. The simulation results show that parameters such as P_s, $P_{\min}$, P_{th} and α which affect the transmission power of the relay node, also have an impact on the system's outage probability. Furthermore, the power parameter P_s of the energy source has the most significant

influence on the system's outage probability. In high SNR scenarios, a tenfold increase in P_s results in a nearly 90% reduction in the system's outage probability. We also conclude that the proposed XOR system is much better than the conventional NXOR system in terms of intercept performance in the case of without significantly reducing the outage performance, which indicates the advantage of the proposed protocol. Additionally, the security performance of the system is closely tied to the CSI from the signal source to the eavesdropper. It can be seen that the smaller the probability that the eavesdropper successfully obtains the key provided by the energy source, the safer the data exchanged between the two users.

In conclusion, this research demonstrates that signal sources also have great potential to enhance system security. This finding holds particular relevance in practical application scenarios, including the internet of things, military communications, and autonomous sensor networks, where energy sources are inherently indispensable. Employing an external energy source as an encryption signal source can effectively fortify system security. Consequently, this study lays the foundation for future investigations in the domain of security for energy-constrained systems. As for future work, how to prevent the signal sent by the energy source from being successfully decoded is a critical issue to be addressed in the next step.

REFERENCES

[1] C. E. García, M. R. Camana, and I. Koo, "Low-complexity PSO-based resource allocation scheme for cooperative non-linear SWIPT-enabled NOMA," *IEEE Access*, vol. 10, pp. 34207–34220, 2022.

[2] M.-L. Ku, W. Li, Y. Chen, and K. J. Ray Liu, "Advances in energy harvesting communications: Past, present, and future challenges," *IEEE Commun. Surveys Tuts.*, vol. 18, no. 2, pp. 1384–1412, 2nd Quart., 2016.

[3] A. Rajaram, R. Khan, S. Tharranetharan, D. Jayakody, R. Dinis, and S. Panic, "Novel SWIPT schemes for 5G wireless networks," *Sensors*, vol. 19, no. 5, p. 1169, Mar. 2019.

[4] D. Ma, G. Lan, M. Hassan, W. Hu, and S. K. Das, "Sensing, computing, and communications for energy harvesting IoTs: A survey," *IEEE Commun. Surveys Tuts.*, vol. 22, no. 2, pp. 1222–1250, 2nd Quart., 2020.

[5] Y. Guo, X. Liu, X. Liu, and T. S. Durrani, "Energy-efficient resource allocation for simultaneous wireless information and power transfer in GFDM cooperative communications," *IEEE Netw. Lett.*, vol. 4, no. 1, pp. 1–5, Mar. 2022.

[6] O. Alamu, T. O. Olwal, and K. Djouani, "Achievable rate optimization for space–time block code-aided cooperative NOMA with energy harvesting," *Eng. Sci. Technol., Int. J.*, vol. 40, Apr. 2023, Art. no. 101365. [Online]. Available: https://www.sciencedirect.com/science/article/pii/S2215098623000423

[7] T. D. Ponnimbaduge Perera, D. N. K. Jayakody, S. K. Sharma, S. Chatzinotas, and J. Li, "Simultaneous wireless information and power transfer (SWIPT): Recent advances and future challenges," *IEEE Commun. Surveys Tuts.*, vol. 20, no. 1, pp. 264–302, 1st Quart., 2018.

[8] T. A. Zewde and M. C. Gursoy, "NOMA-based energy-efficient wireless powered communications," *IEEE Trans. Green Commun. Netw.*, vol. 2, no. 3, pp. 679–692, Sep. 2018.

[9] L. Ma, E. Li, and Q. Yang, "On the performance of full-duplex cooperative NOMA with non-linear EH," *IEEE Access*, vol. 9, pp. 145968–145976, 2021.

[10] M. Maleki, A. M. D. Hoseini, and M. Masjedi, "Performance analysis of SWIPT relay systems over Nakagami-*m* fading channels with non-linear energy harvester and hybrid protocol," in *Proc. Electr. Eng. (ICEE), Iranian Conf.*, Iran, May 2018, pp. 610–615.

[11] A. A. Okandeji, M. R. A. Khandaker, K.-K. Wong, G. Zheng, Y. Zhang, Z. Zheng, and R. Liu, "SWIPT in MISO full-duplex systems," *J. Commun. Netw.*, vol. 19, no. 5, pp. 470–480, Oct. 2017.

[12] E. Boshkovska, D. W. K. Ng, N. Zlatanov, and R. Schober, "Practical non-linear energy harvesting model and resource allocation for SWIPT systems," *IEEE Commun. Lett.*, vol. 19, no. 12, pp. 2082–2085, Dec. 2015.

[13] L. Zhang, J. Zhang, N. Hu, X. Li, and G. Pan, "Outage performance for NOMA-based FSO-RF systems with transmit antenna selection and nonlinear energy harvesting," *IEEE Internet Things J.*, vol. 10, no. 7, pp. 6491–6506, Apr. 2023.

[14] J. Zhang, L. Zhang, and G. Pan, "Outage performance for NOMA-based FSO-RF systems with a dual energy harvesting mode," *IEEE Internet Things J.*, vol. 10, no. 18, pp. 16076–16086, Sep. 2023.

[15] R. Jiang, K. Xiong, P. Fan, Y. Zhang, and Z. Zhong, "Power minimization in SWIPT networks with coexisting power-splitting and time-switching users under nonlinear EH model," *IEEE Internet Things J.*, vol. 6, no. 5, pp. 8853–8869, Oct. 2019.

[16] U. Makhanpuri, K. Agrawal, A. Jee, and S. Prakriya, "Performance of full-duplex cooperative NOMA network with nonlinear energy harvesting," in *Proc. IEEE 32nd Annu. Int. Symp. Pers., Indoor Mobile Radio Commun. (PIMRC)*, Sep. 2021, pp. 495–500.

[17] P. Maji, S. D. Roy, and S. Kundu, "Physical layer security with non-linear energy harvesting relay," in *Proc. 10th Int. Conf. Comput., Commun. Netw. Technol. (ICCCNT)*, Jul. 2019, pp. 1–6.

[18] B. Chen, R. Li, Q. Ning, K. Lin, C. Han, and V. C. M. Leung, "Security at physical layer in NOMA relaying networks with cooperative jamming," *IEEE Trans. Veh. Technol.*, vol. 71, no. 4, pp. 3883–3888, Apr. 2022.

[19] Y. Wu, G. Ji, T. Wang, L. Qian, B. Lin, and X. Shen, "Non-orthogonal multiple access assisted secure computation offloading via cooperative jamming," *IEEE Trans. Veh. Technol.*, vol. 71, no. 7, pp. 7751–7768, Jul. 2022.

[20] Z. Tang, T. Hou, Y. Liu, J. Zhang, and L. Hanzo, "Physical layer security of intelligent reflective surface aided NOMA networks," *IEEE Trans. Veh. Technol.*, vol. 71, no. 7, pp. 7821–7834, Jul. 2022.

[21] D. W. K. Ng, E. S. Lo, and R. Schober, "Robust beamforming for secure communication in systems with wireless information and power transfer," *IEEE Trans. Wireless Commun.*, vol. 13, no. 8, pp. 4599–4615, Aug. 2014.

[22] Z. Hu, D. Xie, M. Jin, L. Zhou, and J. Li, "Relay cooperative beamforming algorithm based on probabilistic constraint in SWIPT secrecy networks," *IEEE Access*, vol. 8, pp. 173999–174008, 2020.

[23] L. Dong, Z. Han, A. P. Petropulu, and H. V. Poor, "Improving wireless physical layer security via cooperating relays," *IEEE Trans. Signal Process.*, vol. 58, no. 3, pp. 1875–1888, Mar. 2010.

[24] X. Lu, P. Wang, D. Niyato, D. I. Kim, and Z. Han, "Wireless networks with RF energy harvesting: A contemporary survey," *IEEE Commun. Surveys Tuts.*, vol. 17, no. 2, pp. 757–789, 2nd Quart., 2015.

[25] M. R. A. Khandaker, C. Masouros, K.-K. Wong, and S. Timotheou, "Secure SWIPT by exploiting constructive interference and artificial noise," *IEEE Trans. Commun.*, vol. 67, no. 2, pp. 1326–1340, Feb. 2019.

[26] M. M. Salim, H. A. Elsayed, M. A. Elaziz, M. M. Fouda, and M. S. Abdalzaher, "An optimal balanced energy harvesting algorithm for maximizing two-way relaying D2D communication data rate," *IEEE Access*, vol. 10, pp. 114178–114191, 2022.

[27] S. Silva, G. A. A. Baduge, M. Ardakani, and C. Tellambura, "NOMA-aided multi-way massive MIMO relaying," *IEEE Trans. Commun.*, vol. 68, no. 7, pp. 4050–4062, Jul. 2020.

[28] X. Li, Q. Wang, Y. Liu, T. A. Tsiftsis, Z. Ding, and A. Nallanathan, "UAV-aided multi-way NOMA networks with residual hardware impairments," *IEEE Wireless Commun. Lett.*, vol. 9, no. 9, pp. 1538–1542, Sep. 2020.

[29] D. Kumar, P. K. Singya, J. Nebhen, and V. Bhatia, "Performance of SWIPT-enabled FD TWR network with hardware impairments and imperfect CSI," *IEEE Syst. J.*, vol. 17, no. 1, pp. 1224–1234, Mar. 2023.

[30] M. M. Salim, H. A. Elsayed, M. S. Abdalzaher, and M. M. Fouda, "RF energy harvesting dependency for power optimized two-way relaying D2D communication," in *Proc. IEEE Int. Conf. Internet Things Intell. Syst. (IoTaIS)*, Nov. 2022, pp. 297–303.

[31] W. Wang, R. Wang, H. Mehrpouyan, N. Zhao, and G. Zhang, "Beamforming for simultaneous wireless information and power transfer in two-way relay channels," *IEEE Access*, vol. 5, pp. 9235–9250, 2017.

[32] K. Xiong, Y. Zhang, Y. Chen, and X. Di, "Power splitting based SWIPT in network-coded two-way networks with data rate fairness: An information-theoretic perspective," *China Commun.*, vol. 13, no. 12, pp. 107–119, Dec. 2016.

[33] S. T. Shah, D. Munir, M. Y. Chung, and K. W. Choi, "Information processing and wireless energy harvesting in two-way amplify-and-forward relay networks," in *Proc. IEEE 83rd Veh. Technol. Conf. (VTC Spring)*, May 2016, pp. 1–5.
[34] T. P. Do, I. Song, and Y. H. Kim, "Simultaneous wireless transfer of power and information in a decode-and-forward two-way relaying network," *IEEE Trans. Wireless Commun.*, vol. 16, no. 3, pp. 1579–1592, Mar. 2017.
[35] E. Li, S. Yang, and H. Wu, "A source-relay selection scheme in two-way amplify-and-forward relaying networks," *IEEE Commun. Lett.*, vol. 16, no. 10, pp. 1564–1567, Oct. 2012.

ENYU LI (Member, IEEE) received the B.Eng. degree in electronic information engineering from Shandong Normal University, Jinan, China, in 2005, the M.Eng. degree in pattern recognition and intelligent systems from the Sichuan University of Science and Engineering, Zigong, China, in 2009, and the Ph.D. degree in communication and information system from Chongqing University, Chongqing, China, in 2013.

He is currently an Associate Professor with the Qingdao University of Technology, Qingdao, China. His current research interests include cooperative communications and physical-layer security, energy harvesting, and intelligent reflecting surface.

YE WANG received the B.Eng. degree in communication engineering from the Shandong University of Science and Technology, Qingdao, China, in 2019. He is currently pursuing the M.Eng. degree in electronic information with the School of Information and Control Engineering, Qingdao University of Technology, Qingdao.

His current research interests include cooperative communications, non-orthogonal multiple access, and physical-layer security.

ZANYANG LIANG received the B.Eng. degree in communication engineering from Tianjin Normal University, Tianjin, China, in 2020. She is currently pursuing the M.Eng. degree in information and communication engineering with the Qingdao University of Technology, Qingdao, China.

Her current research interests include cooperative communications, non-orthogonal multiple access, physical-layer security, and energy harvesting.

MEIJUAN ZHENG received the B.Eng. degree in electronic information science and technology from Qufu Normal University, China, in 2021. She is currently pursuing the M.Eng. degree in electronic information with the School of Information and Control Engineering, Qingdao University of Technology, Qingdao, China.

Her current research interests include cooperative communications, energy harvesting, and physical-layer security.